Journal of Advanced Research xxx (xxxx) xxx

Contents lists available at ScienceDirect

Journal of Advanced Research

journal homepage: www.elsevier.com/locate/jare

Original Manuscript

Beaver behavior optimizer: A novel metaheuristic algorithm for solar PV parameter identification and engineering problems

Kaichen Ouyang [a,1], Dedai Wei [b,1], Xinye Sha [c], Juntao Yu [a], Yuanli Zhao [d], Minyu Qiu [e], Shengwei Fu [f], Ali Asghar Heidari [g], Huiling Chen [d,*]

[a] Department of Mathematics, University of Science and Technology of China, Hefei 230026, China
[b] College of Economics, Shenyang University, Shenyang 110000, China
[c] Graduate School of Arts and Sciences, Columbia University, NY 10027, United States
[d] Institute of Big Data and Information Technology, Wenzhou University, Wenzhou 325000, China
[e] China Jiliang University Information Engineering College Hangzhou, Zhejiang, China
[f] Key Laboratory of Advanced Manufacturing Technology, Ministry of Education, Guizhou University, Guiyang, Guizhou 550025, China
[g] School of Surveying and Geospatial Engineering, College of Engineering, University of Tehran, Tehran, Iran

HIGHLIGHTS

- This study proposed a novel metaheuristic algorithm called BBO.
- BBO was evaluated on CEC 2017 and CEC 2022 benchmark suites.
- BBO outperformed 11 algorithms in terms of convergence and robustness.
- BBO was applied to solve 3 solar PV parameter identification problems.
- BBO was utilized to address 4 complex real-world engineering challenges.

GRAPHICAL ABSTRACT

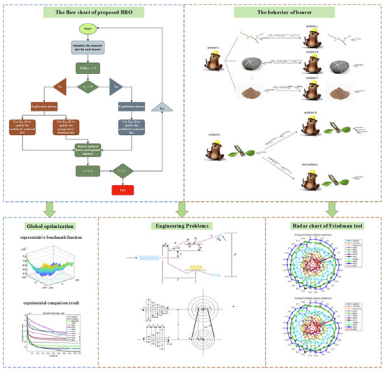

ARTICLE INFO

Article history:
Received 10 November 2024
Revised 26 August 2025
Accepted 1 September 2025
Available online xxxx

Keywords:
Solar PV parameter
Engineering problems
Swarm intelligence
Beaver behavior optimizer (BBO)
Numerical optimization

ABSTRACT

Introduction: Numerical optimization plays a key role in improving the efficiency of solar photovoltaic (PV) systems and solving complex engineering problems. Traditional optimization methods often struggle with finding optimal solutions within a reasonable timeframe due to high-dimensional and nonlinear problem landscapes.
Objectives: This study aims to introduce a novel swarm intelligence algorithm, the Beaver Behavior Optimizer (BBO), inspired by the cooperative behaviors of beavers during dam construction. The goal is to validate BBO's performance on both benchmark test functions and real-world engineering problems, particularly in solar PV parameter optimization.
Methods: The BBO was modeled based on beaver behaviors of material gathering and dam maintenance, integrating exploration and exploitation phases. To assess its performance, experiments were conducted using CEC 2017 and CEC 2022 benchmark functions with varying dimensions (10, 20, 30, 50, 100). Statistical significance was verified using Wilcoxon signed-rank and Friedman mean rank tests.

* Corresponding author.
E-mail addresses: oykc@mail.ustc.edu.cn (K. Ouyang), wdd31212@163.com (D. Wei), xs2399@columbia.edu (X. Sha), tomsnake@mail.ustc.edu.cn (J. Yu), yuanli_wzu@126.com (Y. Zhao), vpn2733@autuni.ac.nz (M. Qiu), shengwei_fu@163.com (S. Fu), aliasghar68@gmaill.com (A.A. Heidari), chenhuiling_jsj@wzu.edu.cn (H. Chen).
[1] Kaichen OuYang and Dedai Wei contributed equally to this work.

https://doi.org/10.1016/j.jare.2025.09.001

Furthermore, BBO was applied to solve three solar PV parameter identification problems and four real-world engineering problems, comparing its performance with 11 other algorithms.
Results: BBO demonstrated superior performance across all benchmark functions and ranked first in tackling solar PV and engineering design problems. It outperformed other state-of-the-art algorithms in most test scenarios, showcasing robust convergence, quick optimization, and minimal variance in results.
Conclusion: The results validate BBO as a powerful optimization tool, particularly for solar PV parameter identification and engineering challenges. Its bio-inspired approach effectively balances exploration and exploitation, making it a competitive algorithm for solving complex optimization tasks.The source code of BBO is available at: https://github.com/oykc1234/BBO.

Introduction

Photovoltaic (PV) systems and engineering design problems share a common challenge: optimizing parameters to enhance the efficiency and economic benefits of their respective systems. The PV system's efficiency and economic viability are contingent upon module-specific attributes such as type, efficiency, and temperature response, as well as broader system considerations including array setup, orientation, and potential shading influences. In the parallel domain of engineering design, material choices, structural configurations, load distributions, and manufacturing techniques are pivotal, dictating the cost-effectiveness, operational performance, and durability of the end product [1–6].

Solving these problems usually means finding the maximum or minimum value of an objective function while meeting certain constraints [7–11]. However, their complex nature creates challenges for traditional optimization methods. These challenges include high-dimensional search spaces, functions that aren't smooth or differentiable, and many local optimal solutions that can trap algorithms [12]. Metaheuristic algorithms (MAs), drawing inspiration from natural phenomena, offer a powerful alternative for addressing these challenges. Unlike deterministic methods, which may struggle with complex landscapes and require gradient information, MAs navigate the search space stochastically, allowing for a more flexible exploration. MAs are particularly adept at avoiding local optima, a common pitfall in optimization tasks, by employing mechanisms like population diversity and adaptive behavior to balance exploration (searching new areas of the search space) and exploitation (refining solutions within promising areas). This enables them to effectively converge towards global optima even in the absence of explicit problem structures or derivative information [13–15].

MAs are typically grouped into four main categories: swarm intelligence algorithms(SIAs), physics-based algorithms (PBAs), evolutionary algorithms (EAs), and human-based algorithms (HBAs) [8]. SIAs are particularly notable for their emulation of collective natural behaviors, such as the coordination seen in bird swarms. This category includes the well-known particle swarm optimization (PSO), which has been the subject of extensive research and application [16]. PBAs, meanwhile, are inspired by principles of physics and chemical processes, exemplified by the simulated annealing algorithm, which is based on the metallurgical technique of annealing [17]. EAs draw on the concepts of biological evolution, with the genetic algorithm (GA) being a primary example that simulates natural selection and genetic inheritance [18]. Finally, HBAs aim to mimic human cognitive and social processes, with the teaching–learning-based optimization (TLBO) algorithm replicating the interaction dynamics of a classroom setting [19]. This study will mainly focus on SIAs, highlighting their unique approach to problem-solving by leveraging the collective behaviors observed in nature.

SIAs, a prominent class of MAs, derives its principles from the natural collective behaviors observed in biological systems such as insect swarms and bird flocks [20]. Since 1990 s, SIAs has evolved from tackling functional optimization tasks to a wide array of applications across various disciplines [21]. Algorithms like PSO [16] and ant colony optimization (ACO) [22] demonstrate SIAs' capability in complex problem-solving by balancing exploration and exploitation, thus avoiding local optima and ensuring convergence towards optimal solutions [23]. Beyond functional optimization, SIAs' adaptability is showcased in microgrid optimal dispatching [24], in robot path planning [25], and in feature selection [26]. Furthermore, SIAs has made significant contributions in solving combinatorial problems like the traveling salesman problem [27], illustrating its versatility and efficacy in addressing computational challenges. The continuous development of new algorithms and hybrid approaches within SIAs broadens its application spectrum, emphasizing its role as a dynamic and flexible tool in computational optimization [28–31]. As SIAs progresses, its potential for innovative solutions across a myriad of fields is increasingly recognized, underscoring its importance in the realm of MAs.

The no free lunch (NFL) theorem underscores the idea that no single algorithm outperforms all others across every possible scenario, highlighting the continuous need for developing novel algorithms [32]. This approach not only expands the repertoire of available algorithms but also ensures that for any given problem, the most suitable and efficient algorithm can be identified and applied. Solar PV problems are the key part of solar energy capture. Many researchers are keen on enhancing the efficiency and effectiveness of this task, which can contribute to the broader utilization of renewable energy sources [33]. Optimization algorithms often struggle with solar PV problems due to the nonlinear, dynamic nature of solar systems and the high-dimensional, computationally intensive nature of the optimization tasks [34–38]. To solve Solar PV and other engineering problems more efficiently, an innovative SIA called Beaver Behavior Optimizer (BBO) is introduced in this work. This algorithm is designed to excel in numerical optimization tasks, including the precise identification of parameters in solar PV systems and the optimization of complex engineering problems. BBO introduces a fresh perspective to SI, inspired by beavers' sophisticated dam construction abilities. Beavers are natural engineers, skillfully altering their environment to create calm water habitats, a trait that underpins the BBO. This method leverages the collective, strategic efforts of beaver-like agents for resource gathering and utilization, targeting the efficient exploration and exploitation of the solution space. It effectively addresses challenges such as sensitivity to starting conditions, quick convergence to suboptimal solutions, and local optimum stagnation that affect many traditional algorithms. By emulating the beavers' methodical approach to scouting, building, and maintenance, the BBO ensures a balanced search strategy, leading to the identification of optimal solutions across a variety of problem domains. This paper makes substantial contributions in several key areas:

1. An efficient optimizer, BBO for various optimization cases is proposed.
2. The construction of an efficient optimization mechanism in BBO is characterized by its a clear distinction between the exploration and exploitation phase and enhanced optimization capabilities. The innovation of this paper lies in simulating the dam construction behavior of beavers, getting inspiration from the cooperative behavior in the process of material collection and dam maintenance, building a mathematical model, and constantly upgrading and improving it. Through experiments, the excellent performance of BBO is verified, so that it can be used to solve real world problems.
3. Validation of the algorithm's performance through comparative experiments with 11 mature algorithms demonstrates strong competitiveness of the BBO in CEC benchmark functions.
4. BBO is applied to one solar PV and four real-world engineering design problems substantiates its potential to address a wide range of practical optimization tasks.

The remainder of this document is structured as follows: The inspiration behind BBO and its mathematical framework are outlined in **Section 2**. Numerical experiments are carried out and thoroughly analyzed in **Section 3**. **Section 4** demonstrates the application of BBO in identifying parameters for three photovoltaic models. In **Section 5**, BBO is employed to tackle four distinct engineering design issues. A summary of this research and considerations for future work are discussed in **Section 6**.

The beaver behavior optimizer (BBO)

Inspiration

The BBO draws its inspiration from the exceptional dam-building activities of beavers, widely recognized for their environmental engineering capabilities [39–41]. These animals, primarily found across North America and parts of Eurasia, exhibit a unique blend of social behavior, strategic planning, and environmental manipulation that serves as the foundation for this innovative optimization approach. Beavers are known for their ability to construct elaborate dams across streams and rivers, creating still-water environments that serve both as their habitat and as protection against predators. The construction process involves the collective efforts of beaver families, which work together to gather wood, stones, and mud [42]. These materials are meticulously selected and strategically placed to ensure the structural integrity and functionality of the dam. The beavers' construction behavior is marked by several key phases. Initially, beavers scout for suitable locations, considering factors such as water flow and surrounding vegetation. Once a site is chosen, beavers collectively transport materials, using their sharp teeth to cut trees and branches, which are then interwoven with mud to form the dam's foundation [43]. Throughout this process, beavers demonstrate a remarkable ability to adapt their construction techniques to the changing environment, ensuring the dam's continuous maintenance and improvement. Moreover, beavers exhibit an ability to store food for the winter months by creating underwater food caches near their lodges, showcasing foresight and planning [44]. This aspect of their behavior highlights their strategic resource management, an element mirrored in the BBO's emphasis on efficient resource allocation and problem-solving. By emulating the beavers' construction ingenuity, social cooperation, and adaptive strategies, the BBO introduces a novel approach to optimization. It incorporates phases of exploration and exploitation, analogous to the beavers' scouting and building activities, ensuring a thorough search of the solution space and the efficient identification of optimal solutions. This inspiration from nature not only enhances the understanding of swarm intelligence but also provides a robust framework for tackling complex optimization challenges across various domains.

Population initialization

In BBO, every dimension j of the individual is analogous to a type of construction material, like branches or stones, with its corresponding value reflecting the material's property. The individuals within the population symbolize the unique assortment of materials possessed by each beaver. At the onset, through a process depicted in Eq. (1), each beaver is endowed with a randomly assorted set of materials, each varying in properties. As shown in Fig. 1, two beavers use different materials to build their habitats

$$M = \begin{bmatrix} m_{1,1} & \cdots & m_{1,j} & \cdots & m_{1,D-1} & m_{1,D} \\ m_{2,1} & \cdots & m_{2,j} & \cdots & \cdots & m_{2,D} \\ \cdots & \cdots & m_{i,j} & \cdots & \cdots & \cdots \\ \vdots & \vdots & \vdots & \vdots & \vdots & \vdots \\ m_{n-1,1} & \cdots & m_{n-1,j} & \cdots & \cdots & m_{n-1,D} \\ m_{n,1} & \cdots & m_{n,j} & \cdots & m_{n,D-1} & m_{n,D} \end{bmatrix} \tag{1}$$

where M represents the state matrix of the material held by beavers in the population, $m_{i,j}$ represents the properties of the j^{th} material held by the i^{th} beaver, n represents the number of beaver species in the population, and D represents the type of materials.

$$m_{i,j} = (ub_j - lb_j) \times rand + lb_j \tag{2}$$

where lb_j and ub_j represent the lower bound and upper bound of the property change of the j-th material, and $rand$ represents a variable that changes from 0 to 1.

Dam-Phase factor

During the beaver dam construction process, the early stage involves material collection. At this point, beavers scout different locations for potential dam construction sites while actively seeking suitable materials. In the later stages, beavers focus on maintaining and refining the formed dam. These behaviors of beavers correspond precisely to the exploration and exploitation stages in MAs. To mathematically model this behavioral transition, the dam-phase factor D is introduced, as defined in Eq. (3), where t represents the current iteration count and T denotes the maximum number of iterations. The factor D increases monotonically from 0 to 1 throughout the optimization process.

$$D = sin\left(\frac{\pi t}{2T}\right) \tag{3}$$

At each iteration, a random number r_1 uniformly distributed in [0,1] is generated to determine whether the population enters exploitation (when $r_1 \leq D$) or exploration phase. This mechanism ensures that while the algorithm gradually shifts focus toward exploitation in later iterations, it always maintains the possibility of exploration – accurately reflecting how beavers primarily maintain established dams in later phases while remaining capable of seeking better locations. The dam-phase factor effectively enhances the algorithm's randomness, prevents premature convergence, and optimally balances exploration and exploitation throughout the search process.

Exploration phase: Material gathering behavior of beavers

In the exploration phase, the material gathering behavior of beavers are modeled. In this phase, the beaver population is

Fig. 1. Two beavers are using different materials.

divided into two types: architects and prospectors. The architects are the top 25 % of the population with the most suitable fitness, representing the elite individuals in the population, who carry high-quality materials. The architect will randomly select a fellow architect and learn from him with a 50 % chance to optimize the properties of this material, so that better materials can be added to the architect's dam construction. The mutual learning behavior of architects can be described by Eq. (4). If it is a prospector, for each material j, it will randomly select an architect from the population and learn from him with a 50 % probability of that material type to optimize its own material j. At the same time, prospectors will actively explore different materials j to optimize existing materials. The prospector's updated formula during the exploration phase is described by Eq. (5).

$$m_{i,j}^{architect}(t+1) = m_{i,j}^{architect}(t) + I(r_2 < 0.5) r_3 \left(m_{k,j}^{architect}(t) - m_{i,j}^{architect}(t) \right) \quad (4)$$

$$m_{i,j}^{prospedor}(t+1) = m_{i,j}^{prospedor}(t) + I(r_4 < 0.5) r_5 \left(m_{i,j}^{architect}(t) - m_{i,j}^{prospector}(t) \right) + \frac{r_6 cos\left(\frac{\pi t}{2T}\right)(ub_j - lb_j)}{10} \quad (5)$$

In Eq. (4), the updated formula for the architect in the exploration phase is described, where $m_{i,j}^{architect}(t)$ represents the properties of the j-th material for the i architect at the t iteration. $I(x)$ is a characteristic function. When the logic of x is true, the value of the function is 1, and vice versa, it is 0. $m_{k,j}^{architect}$ represents the properties of the j-th material of the architect k, other than architect i, randomly selected from the population. r_2 and r_3 are random numbers between 0 and 1 generated by uniform distribution. In Eq. (5), $m_{i,j}^{prospedor}(t)$ represents the properties of the j material in the t iteration of the i prospector, r_4 and r_5 are two random numbers within [0,1] generated by a uniform distribution, and the last term of the Eq. (5) represents the beaver's random exploration of the properties of the j-th material in order to find a more suitable new material. where r_6 represents a random number generated by a Gaussian distribution with a mean of 0 and a variance of 1. Fig. 2 and Fig. 3 show the behavior of beaver architects and prospectors during the exploration phase.

Exploitation phase: Dam maintenance and improvement

When the beavers have finished collecting materials, the colony carries out further maintenance and improvement of the currently built dam, at which point each individual in the population can be regarded as an architect beaver. The animals do not travel to new areas to find materials, but improve the existing materials by learning from the individual with the best combination of materials, as well as other colony members. This process is also consistent with the exploitation stage in evolutionary computation, when the population converges near the optimal solution, a fine search will be carried out near the optimal solution, and the optimal solution will be continuously improved and perfected. At this stage, population renewal can be described by Eq. (6).

$$m_{i,j}^{architect}(t+1) = m_{i,j}^{architect}(t) + r_7 \left(m_{k,j}^{architect}(t) - m_{i,j}^{architect}(t) \right) + r_8 \left(m_{best,j}^{architect}(t) - m_{i,j}^{architect}(t) \right) \quad (6)$$

In Eq. (6), r_7 and r_8 represent two random numbers within [0,1] generated by uniform distribution, and $m_{best,j}^{architect}(t)$ represents the properties of the j-th material corresponding to the optimal individual in the population at the t iteration. During the exploitation phase, the population renewal process can be described in Fig. 4.

All in all, the BBO draws inspiration from the natural dam-building activities of beavers, leveraging their environmental engineering capabilities for solving complex optimization problems. Initially, individuals within the BBO framework are assigned random properties, mimicking the varied materials beavers collect for dam construction. The algorithm progresses through exploration and exploitation phases, reflecting beaver behaviors of material collection and dam maintenance. During exploration, the population is divided into architects (elite individuals) and prospectors. Architects optimize their materials through peer learning, while prospectors improve theirs by learning from architects and exploring new resources. The exploitation phase focuses on refining materials by learning from optimal solutions, akin to beavers improving their dam. The BBO encapsulates social cooperation, strategic planning, and environmental adaptation seen in beaver behavior. It balances search diversity and focuses within the solution space, offering a nature-inspired approach to optimization that highlights the potential of leveraging biological behaviors in computational intelligence. In order to show the working mechanism of the beaver optimization algorithm more intuitively, the pseudo-code and flow chart of BBO are shown in Fig. 5 and **Algorithm 1**.

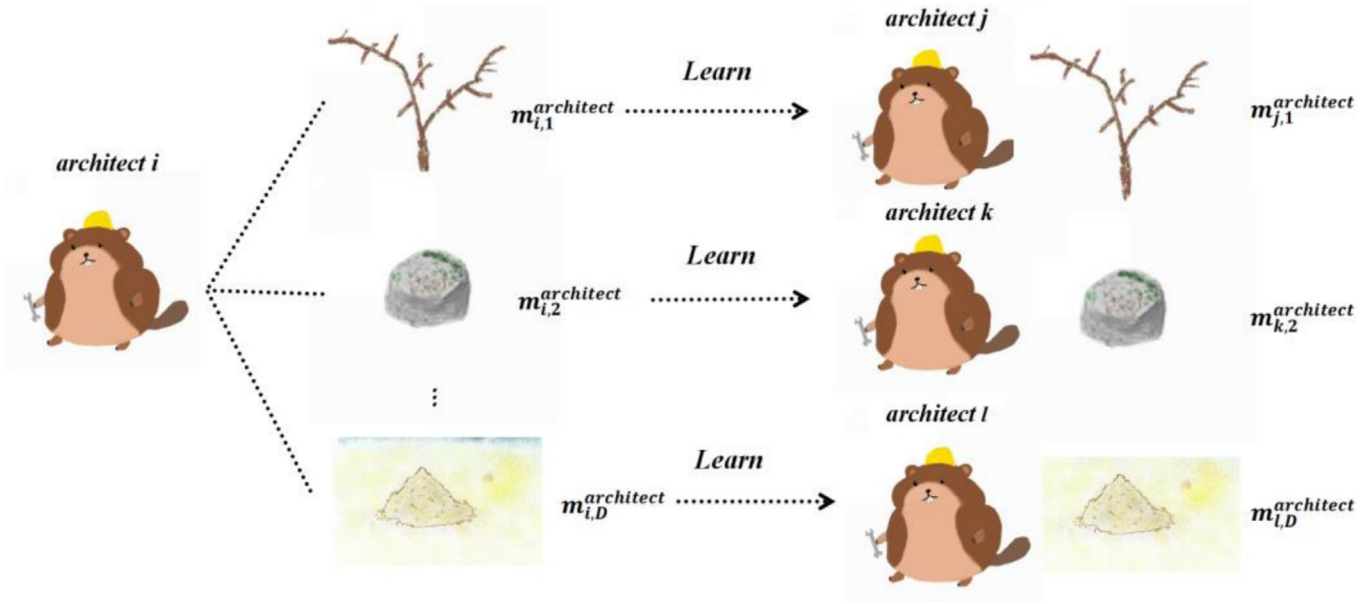

Fig. 2. The behavior of the beaver architect in the exploration phase.

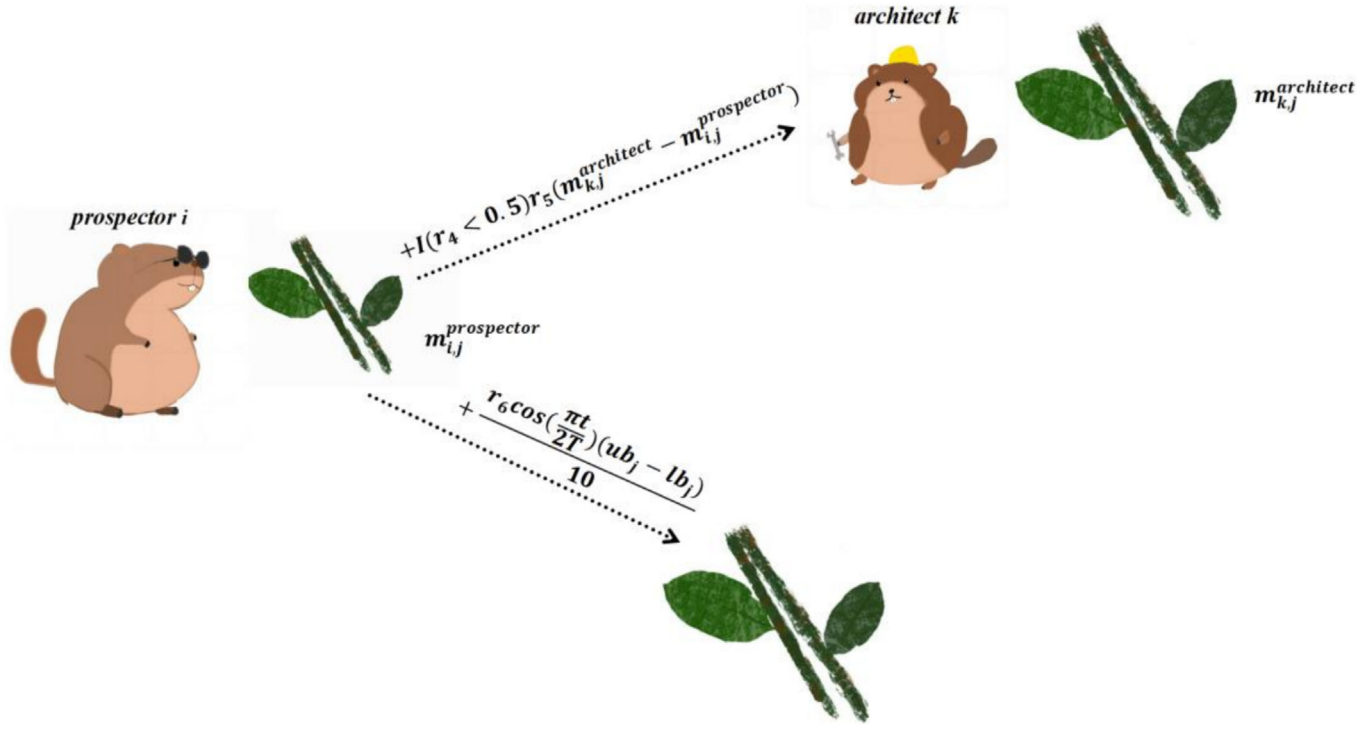

Fig. 3. The behavior of beaver prospectors during the exploration phase.

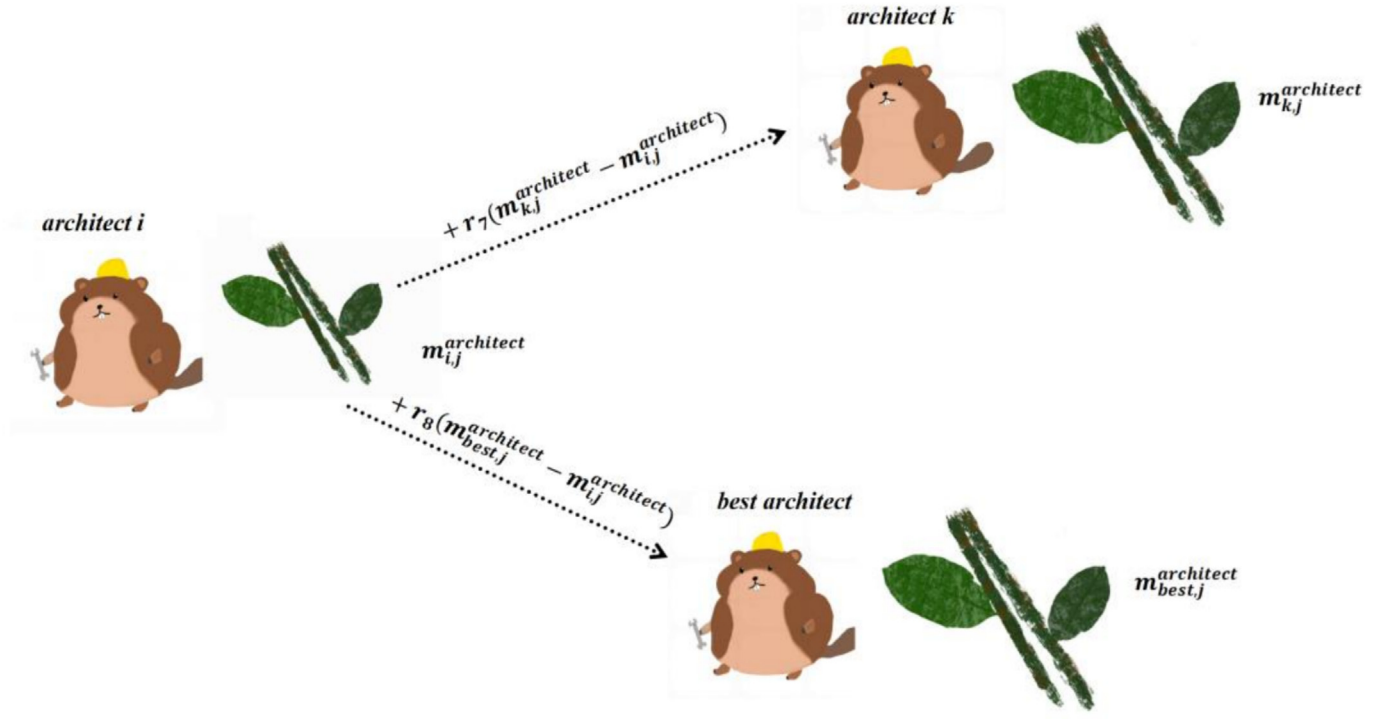

Fig. 4. The architect's updating behavior during the exploitation phase.

Algorithm 1: Pseudo-code of the BBO

```
Initialize the material composition for each beaver
While t<=T
  If r1 ≤ D
    Enter the exploitation phase
    Update the architects' material composition using Eq. (6)
  Else
    Enter the exploration phase
      Divide the population into architects and prospectors
      Update the architects' material composition using Eq. (4)
      Update the prospectors' material composition using Eq. (5)
  End
  Return the optimal fitness and optimal solution of the t iteration
  t = t + 1
End
```

Numerical experiment

This section evaluates the convergence behavior of BBO and compares its performance against 11 other algorithms using the CEC2017 test suite at 30, 50, and 100 dimensions and the CEC2022 test suite at 10 and 20 dimensions. The statistical analysis reports mean values and standard deviations of optimization results from multiple independent runs. For rigorous performance comparison, this section conducted the Wilcoxon signed rank test [45] and Friedman test [46] as nonparametric statistical methods to evaluate algorithmic differences and overall performance.

For the Wilcoxon signed-rank test, when the p-value is less than 0.05, the algorithm is considered to have a significant difference from BBO. Conversely, when the p-value is more than 0.05, there is no significant difference between the two algorithms. The symbols '+/=/−' are used to indicate whether BBO performs better than, similar to, or worse than the competitors. For the Friedman mean rank test, the average rank of each algorithm is computed first and then ranked to determine if there are statistically significant differences among them.

Benchmark test functions

In this section, the performance of the BBO was assessed using the CEC 2017 (Dimensions = 30,50,100) [47] and CEC 2022 (Dimensions = 10,20) benchmarks [48]. For comprehensive evaluation, the experiment employed 30 benchmark functions (F1-F30) from the CEC 2017 test suite and 12 functions (F1-F12) from the CEC 2022 test suite, totaling 42 test functions as shown in Table 1 and Table 2. These functions are categorized based on distinct characteristics and purposes: unimodal functions with a single optimum evaluate the optimization speed and accuracy of an algorithm; multimodal functions, featuring several optima, examine the algorithm's robustness; and hybrid and composition functions challenge the algorithm's capacity to address intricate issues by merging aspects of the first two types. The experiments were conducted on a computer equipped with an Intel Core i5-12400 CPU at 2.50 GHz and 16 GB RAM, utilizing the MATLAB 2023a environment. The experiment parameters are set to 500 iterations with a population size of 30 across all numerical experiments conducted within this section.

Parameters setting for BBO and its competitors

Table 3 illustrates the parameters setting of the BBO and its competitors, including gaussian quantum-behaved particle swarm optimization (GQPSO) [49], terminal crossover and steering-based particle swarm optimization algorithm with disturbance (TCSPSO) [50], memory, evolutionary operator, and local search based

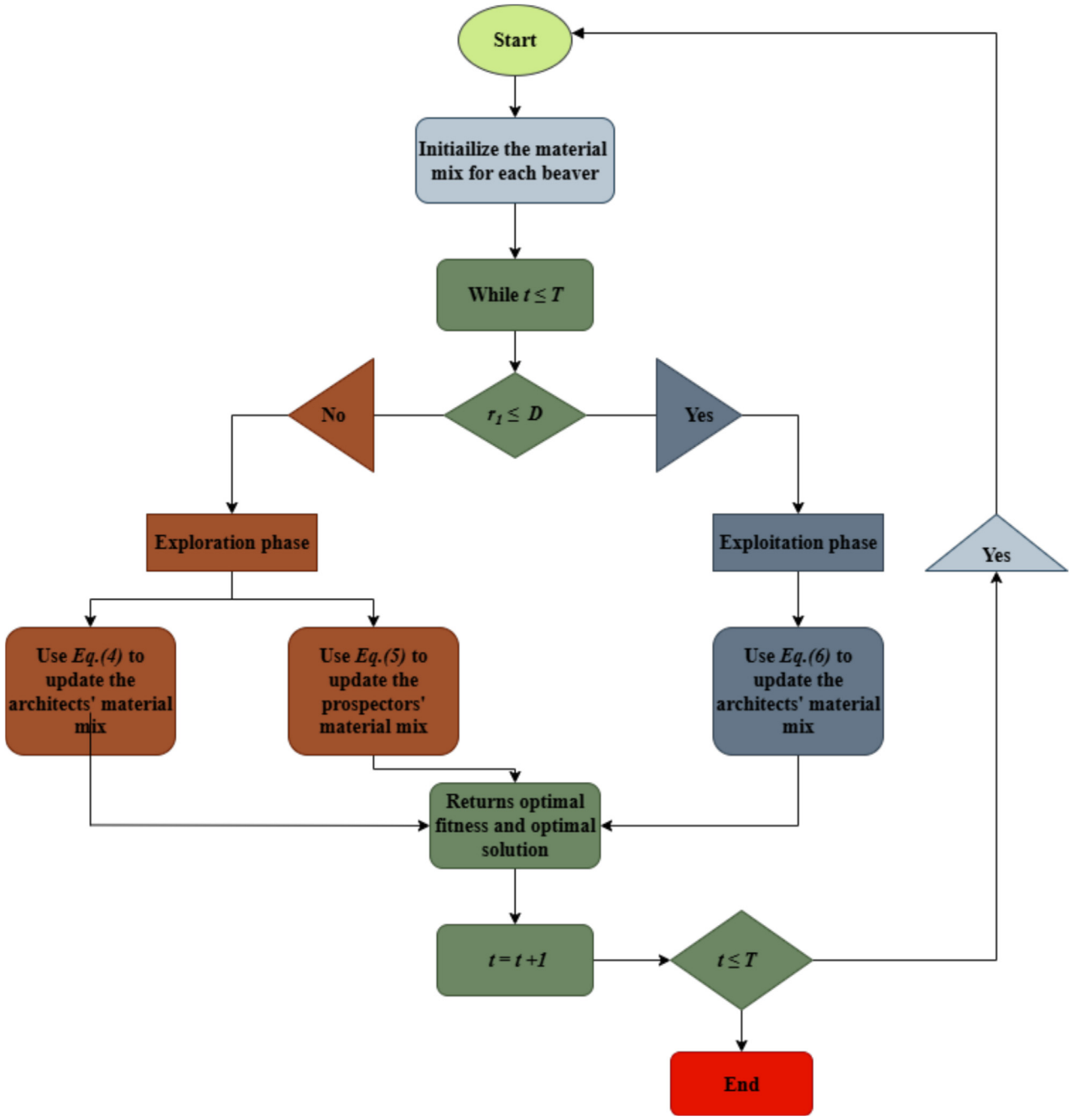

Fig. 5. Flow chart of BBO.

improved grey wolf optimizer (MELGWO) [51], grey wolf optimizer (GWO) [52], Harris hawks optimization (HHO) [12], whale optimization algorithm (WOA) [53], rime optimization algorithm (RIME) [54], crested porcupine optimizer (CPO) [55], Newton-Raphson-based optimizer (NRBO) [56], spider wasp optimizer (SWO) [57], nutcracker optimization algorithm (NOA) [6].

Convergence behavior evaluation

To demonstrate the efficacy of BBO, its convergence characteristics are present in Fig. 6, which contains six graphs illustrating results from various benchmark evaluations. In each graph, the initial column shows the 2D contour of the benchmark function, and the adjacent column illustrates the final positions of the search agents, with the optimal solution indicated by a red dot. These visuals reveal that despite the search agents being dispersed throughout the search space, population predominantly converge around the optimal solution, highlighting BBO's exceptional exploration and exploitation capabilities.

Moreover, the figure's third column depicts the progression of the mean fitness value over iterations. This value starts high but shows a marked decrease, stabilizing after approximately 200 iterations, which evidences BBO's quick convergence ability. The fourth column provides a visual representation of the search agents' movements in the first dimension, showing significant fluctuations in the initial phase of iterations that lessen as the iteration number nears 200. This behavior demonstrates BBO's capacity to avoid local optima and effectively navigate towards global optimization.

Table 1
CEC 2017 benchmark functions.

Type	ID	Description	Dim	f_{min}
Unimodal	F1	Shifted and Rotated Bent Cigar Function	30/50/100	100
	F2	Shifted and Rotated Sum of Different Power Function	30/50/100	200
	F3	Shifted and Rotated Zakharov Function	30/50/100	300
Multimodal	F4	Shifted and Rotated Rosenbrock's Function	30/50/100	400
	F5	Shifted and Rotated Rastrigin's Function	30/50/100	500
	F6	Shifted and Rotated Expanded Scaffer's F6 Function	30/50/100	600
	F7	Shifted and Rotated Lunacek Bi_Rastrigin Function	30/50/100	700
	F8	Shifted and Rotated Non-Continuous Rastrigin's Function	30/50/100	800
	F9	Shifted and Rotated Levy Function	30/50/100	900
	F10	Shifted and Rotated Schwefel's Function	30/50/100	1000
Hybrid	F11	Hybrid Function 1 (N = 3)	30/50/100	1100
	F12	Hybrid Function 2 (N = 3)	30/50/100	1200
	F13	Hybrid Function 3 (N = 3)	30/50/100	1300
	F14	Hybrid Function 4 (N = 4)	30/50/100	1400
	F15	Hybrid Function 5 (N = 4)	30/50/100	1500
	F16	Hybrid Function 6 (N = 4)	30/50/100	1600
	F17	Hybrid Function 6 (N = 5)	30/50/100	1700
	F18	Hybrid Function 6 (N = 5)	30/50/100	1800
	F19	Hybrid Function 6 (N = 5)	30/50/100	1900
	F20	Hybrid Function 6 (N = 6)	30/50/100	2000
Composition	F21	Composition Function 1 (N = 5)	30/50/100	2100
	F22	Composition Function 2 (N = 5)	30/50/100	2200
	F23	Composition Function 3 (N = 5)	30/50/100	2300
	F24	Composition Function 4 (N = 5)	30/50/100	2400
	F25	Composition Function 5 (N = 3)	30/50/100	2500
	F26	Composition Function 6 (N = 3)	30/50/100	2600
	F27	Composition Function 7 (N = 5)	30/50/100	2700
	F28	Composition Function 8 (N = 5)	30/50/100	2800
	F29	Composition Function 9 (N = 5)	30/50/100	2900
	F30	Composition Function 10 (N = 3)	30/50/100	3000
Search Range: [-100,100]^D				

Table 2
CEC 2022 benchmark functions.

Type	ID	Description	Dim	f_{min}
Unimodal Function	F1	Shifted and full Rotated Zakharov Function	10/20	300
Basic Functions	F2	Shifted and full Rotated Zakharov Function	10/20	400
	F3	Shifted and full Rotated Expanded Schaffer's f6 Function	10/20	600
	F4	Shifted and full Rotated Non-Continuous Rastrigin's Function	10/20	800
	F5	Shifted and full Rotated Levy Function	10/20	900
Hybrid Functions	F6	Hybrid Function 1 (N = 3)	10/20	1800
	F7	Hybrid Function 2 (N = 6)	10/20	2000
	F8	Hybrid Function 3 (N = 5)	10/20	2200
Composition Functions	F9	Composition Function 1 (N = 5)	10/20	2300
	F10	Composition Function 2 (N = 4)	10/20	2400
	F11	Composition Function 3 (N = 5)	10/20	2600
	F12	Composition Function 4 (N = 6)	10/20	2700
Search Range: [-100,100]^D				

Table 3
Parameters setting for different algorithms.

Algorithms	Name of the parameter	Value of the parameter
GQPSO [49]	w_1, w_2, c_1, c_2	0.5, 1, 1.5, 1.5
TCSPSO [50]	ω, c_1, c_2	0.9 0.4, 2, 2
MELGWO [51]	P_{min}, θ, c_1	$10, decreasesfrom2to0, 2$
GWO [52]	a_{min}, a_{max}	0, 2
HHO [12]	E_0	$[-1, 1]$
WOA [53]	a, b	$decreasefrom2to0.2$
RIME [54]	w	5
CPO [55]	$Numberofindividuals$	20
NRBO [56]	p, q, CF, ε	$[2, 5], [10, n], [0, 1], 0.5$
SWO [57]	TR, CR, N_m, N	0.3, 0.2, 20, 100
NOA [6]	w_1, w_2, c_1, c_2	0.5, 1, 1.5, 1.5
BBO	/	/

Table 4
Wilcoxon signed-rank test on CEC 2017.

BBO vs.	CEC2017 (Dim = 30)	CEC2017 (Dim = 50)	CEC2017 (Dim = 100)
GQPSO	30/0/0	30/0/0	29/0/1
TCSPSO	23/7/0	26/3/1	29/0/1
MELGWO	29/1/0	29/1/0	29/1/0
GWO	25/5/0	25/4/1	27/3/0
HHO	30/0/0	30/0/0	29/0/1
WOA	30/0/0	30/0/0	30/0/0
RIME	20/10/0	28/2/0	29/1/0
CPO	30/0/0	30/0/0	30/0/0
NRBO	29/1/0	30/0/0	29/0/1
SWO	30/0/0	30/0/0	30/0/0
NOA	30/0/0	30/0/0	30/0/0
Overall	**306/24/0**	**318/10/2**	**321/5/4**

Table 5
Friedman test on CEC 2017.

Suites	CEC 2017					
Dimensions	30		50		100	
Algorithms	Ave. Rank	Overall Rank	Ave. Rank	Overall Rank	Ave. Rank	Overall Rank
GQPSO	8.76	9	8.71	9	8.48	9
TCSPSO	3.31	3	3.50	3	3.94	4
MELGWO	4.18	5	4.13	5	4.49	5
GWO	4.09	4	3.91	4	3.71	3
HHO	6.44	6	5.99	6	5.60	6
WOA	7.83	8	7.69	8	7.56	8
RIME	2.78	2	2.91	2	2.99	2
CPO	10.45	11	10.58	11	10.61	11
NRBO	6.85	7	7.32	7	7.45	7
SWO	10.07	10	10.20	10	10.25	10
NOA	11.32	12	11.46	12	11.52	12
BBO	**1.91**	**1**	**1.59**	**1**	**1.41**	**1**

The last column of the figure illustrates the convergence trajectory. For unimodal functions, this trajectory is relatively smooth, indicating that the optimal values can be systematically approached through iterative refinement. Conversely, for multimodal functions with several local optima, the search process involves consistently circumventing these local maxima to achieve the global optimum, which is depicted by a stepped pattern in the convergence trajectory for these cases.

Quantitative analysis

Comparison with other competitive algorithms on CEC 2017

In this section, the performance of BBO against its competitors are evaluated using the CEC 2017 benchmark suite across 30, 50, and 100 dimensional scenarios. Tables 6–8 present the average values and standard deviations of the optimal solutions obtained by BBO and its competitors over 30 independent runs in different dimensions. Across various functions and dimensions, BBO consistently achieves the smallest mean values and standard deviations in most cases. Other notable performers include RIME, TCSPSO, and MELGWO, which also demonstrate superior performance across different functions, while NRBO shows moderate performance. In contrast, GQPSO, CPO, SWO, and NOA exhibit weaker performance with higher mean values and standard deviations compared to other methods. For specific function categories, in unimodal functions, BBO attains the smallest mean values in nearly all dimensions. It achieves the lowest means for all unimodal functions in 30D and 50D scenarios, while in 100D, TCSPSO outperforms BBO on F3. In multimodal functions, BBO maintains its dominance by achieving the smallest means across most functions in different dimensions. Interestingly, GQPSO records the smallest standard deviations in several cases, yet its mean values remain relatively high, indicating its inability to effectively balance convergence and stability. TCSPSO and RIME also perform exceptionally well in multimodal functions. When it comes to hybrid and composition functions, BBO's superiority becomes even more pronounced as dimensionality increases. Notably, in 100D, BBO achieves the lowest mean values in all instances of these complex functions.

Figs. 7 and 8 illustrate BBO's convergence curves and boxplots for selected functions. Fig. 7 reveals that after an initial rapid decline, BBO enters a plateau phase before accelerating its convergence again, demonstrating its ability to escape local optima during early exploration while efficiently converging near the global optimum. Fig. 8 shows that across different dimensions, BBO's boxplots are positioned lower with narrower spreads compared to other algorithms, reflecting its smaller mean values and standard deviations, consistent with the data in Tables 6–8.

Table 4 presents the results of the Wilcoxon signed-rank test between BBO and its competitors. Across all dimensions and nearly all functions, BBO significantly outperforms GQPSO, MELGWO, HHO, WOA, CPO, NRBO, SWO, and NOA, winning in all 30 comparisons or losing only once against these algorithms. TCSPSO, GWO, and RIME emerge as strong competitors to BBO, but as dimensionality increases, BBO's advantage over them expands. Particularly in 100D, BBO significantly outperforms TCSPSO and RIME in 29 out of 30 cases and GWO in 26 cases.

Table 5 displays the Friedman mean rank test results, where BBO secures the top overall ranking across all dimensions, with Friedman ranks of 1.91, 1.59, and 2.41 in 30D, 50D, and 100D, respectively. RIME consistently ranks second in all dimensions, while TCSPSO and GWO also perform well, securing third and fourth places across different dimensions. In contrast, HHO, WOA, and NRBO occupy mid-tier positions, whereas GQPSO, SWO, and NOA rank at the bottom. Figs. 9a, 9b, and 9c present radar charts of the Friedman test results for 30D, 50D, and 100D, respectively. Consistent with Table 5, these visualizations clearly show BBO occupying the innermost position in all cases, confirming its highest ranking.

Comparison with other competitive algorithms on CEC 2022

This section presents a comprehensive performance evaluation of BBO and its competitors on the CEC2022 benchmark suite under 10-dimensional and 20-dimensional scenarios. Tables 11 and 12 display the mean values and standard deviations obtained by BBO and competing algorithms over 30 independent runs across different functions in both dimensional settings. For basic functions, BBO achieved the smallest mean values in over half of the 10-dimensional cases and in all 20-dimensional instances while maintaining relatively low standard deviations, demonstrating its effectiveness in handling low-dimensional problems and strong exploitation capability. RIME and TCSPSO also showed excellent performance, securing the smallest means in some 10-dimensional functions. In hybrid functions and composition functions, BBO still attained the lowest means and standard deviations in more than half of the cases. As dimensionality increased, RIME's performance improved, approaching BBO's level in 20-dimensional scenarios and even achieving the smallest means in several functions. GQPSO recorded the smallest standard deviations in multiple functions but suffered from higher mean values, placing it in the lower-middle performance tier. Other algorithms either performed moderately or fell far behind BBO.

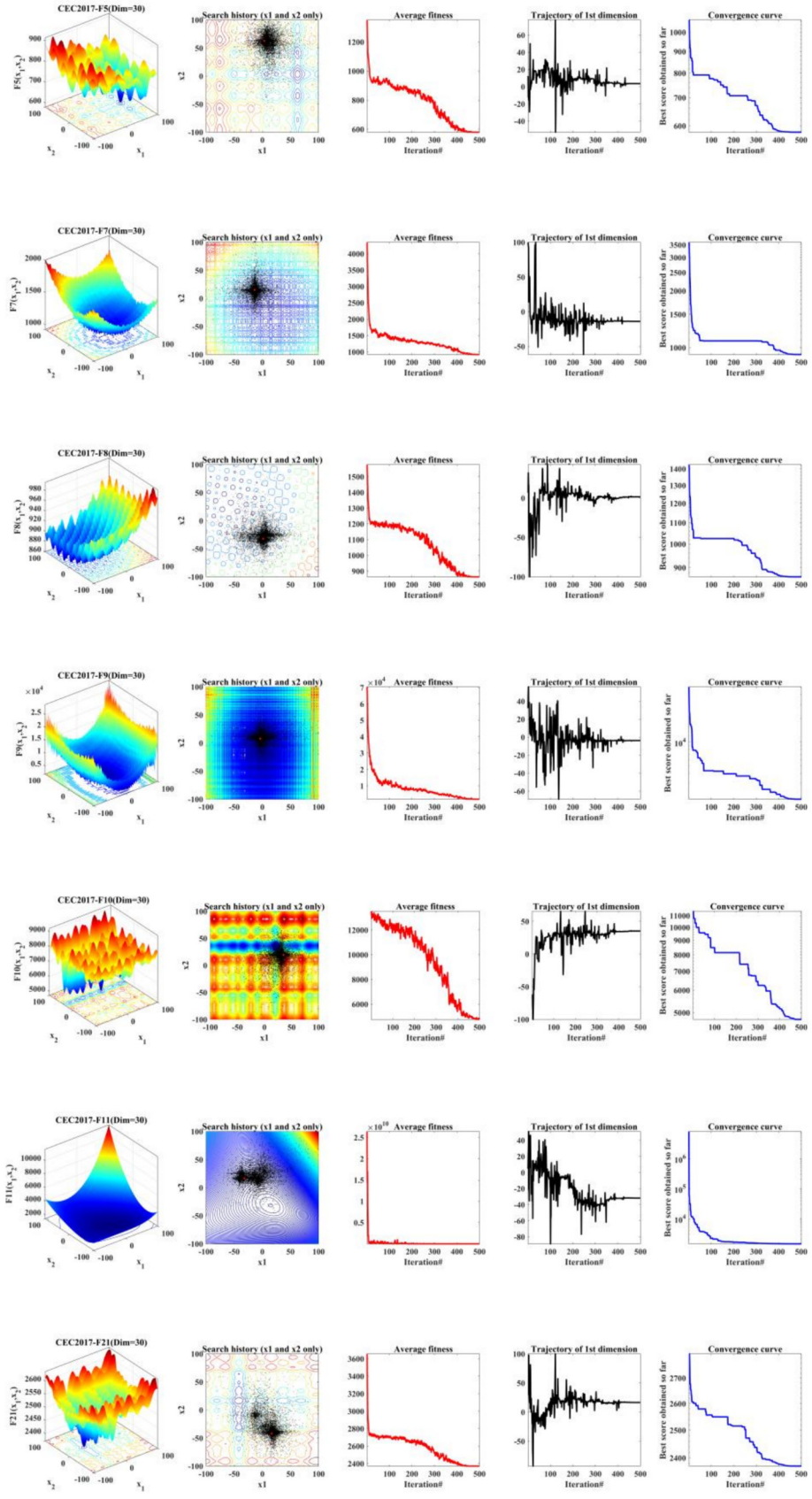

Fig. 6. Convergence behaviors of BBO in the search process.

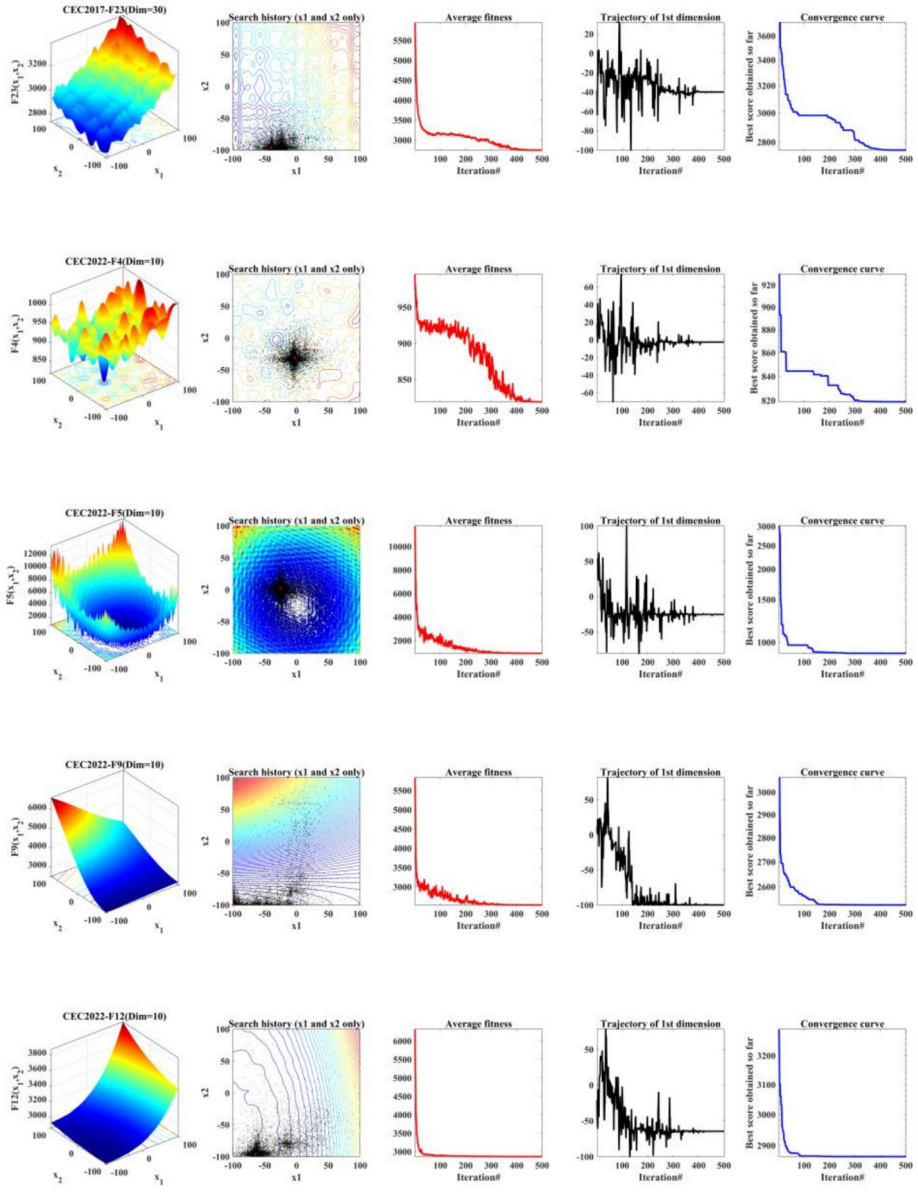

Fig. 6 (*continued*)

Figs. 10 and 11 illustrate the convergence curves and boxplots for selected functions from the CEC2022 test set. In Fig. 10, BBO converges rapidly before stabilizing, highlighting its fast convergence in low-dimensional problems. Fig. 11 shows that BBO's boxplots consistently occupy lower positions with narrower spreads, aligning with the data in Tables 11 and 12 and confirming its superior convergence and stability.

Table 9 presents the Wilcoxon signed-rank test results comparing BBO against its competitors. In 10-dimensional cases, nearly all algorithms were significantly outperformed by BBO, with most losing more than 10 times. HHO was the only exception, losing to BBO 6 times while achieving comparable or better results in 3 instances each. In 20-dimensional scenarios, TCSPSO, GWO, and RIME showed improved performance, matching BBO in 5, 6, and 4 cases respectively, though still falling short overall. Other algorithms remained largely inferior to BBO.

Table 10 displays the Friedman test rankings of BBO and its competitors on the CEC2022 suite. BBO secured the highest overall rankings in both 10D and 20D, followed closely by RIME in second place across all dimensions. TCSPSO, MELGWO, and GWO also performed well, alternating between 3rd, 4th, and 5th places depending on the dimension, while other algorithms ranked significantly lower. Supporting these findings, Figs. 12a and 12b present radar charts of the Friedman test results for 10D and 20D, visually confirming BBO's consistent dominance as it occupies the innermost position in both charts, reflecting its top-tier ranking.

The application of BBO to parameters identification of photovoltaic models

Accurate identification of photovoltaic model parameters is essential for system simulation, performance evaluation, and operational control, relying on measured current–voltage characteristic curves. To achieve fast and accurate identification of parameters for different photovoltaic models, proposed BBO is applied towards three different models, single diode model, double diode model, and PV module Model [58]. For all problems, the parameter settings of BBO and its competitors remain consistent with the previous

Table 6
Experimental results of 12 algorithms on the CEC 2017(Dim = 30).

Algorithm	Metric	GQPSO	TCSPSO	MELGWO	GWO	HHO	WOA	RIME	CPO	NRBO	SWO	NOA	BBO
CEC2017-F1	Avg	2.92677e + 10	3.29028e + 07	1.81671e + 09	2.72677e + 09	3.77859e + 08	4.88966e + 09	4.37268e + 06	3.88972e + 10	1.93288e + 10	3.42314e + 10	7.11142e + 10	**9.83038e + 04**
	Std	1.99612e + 09	2.95936e + 07	1.60521e + 09	1.48514e + 09	1.81684e + 08	1.40677e + 09	1.79803e + 06	6.45600e + 09	4.96490e + 09	7.31207e + 09	6.59553e + 09	**6.61790e + 04**
CEC2017-F2	Avg	1.14674e + 39	2.62111e + 27	2.03642e + 32	9.55351e + 32	1.27115e + 33	1.63067e + 36	1.00740e + 17	6.74483e + 42	2.36646e + 37	1.14645e + 43	2.14662e + 43	**1.64614e + 14**
	Std	3.17655e + 39	1.37570e + 28	9.03487e + 32	5.17529e + 33	4.15018e + 33	6.48215e + 36	2.65588e + 17	2.13903e + 43	1.04990e + 38	4.65292e + 43	3.70596e + 43	**3.62881e + 14**
CEC2017-F3	Avg	7.56991e + 04	3.49609e + 04	4.66176e + 04	6.08159e + 04	5.77598e + 04	2.59362e + 05	4.66034e + 04	1.96048e + 05	5.67684e + 04	1.43994e + 05	1.56322e + 05	**1.82952e + 04**
	Std	**4.60638e + 03**	8.40938e + 03	1.55737e + 04	1.23987e + 04	6.52471e + 03	7.71292e + 04	1.94090e + 04	5.66177e + 04	9.10656e + 03	5.00137e + 04	1.98815e + 04	6.83617e + 03
CEC2017-F4	Avg	5.73777e + 03	5.37949e + 02	6.34551e + 02	6.29687e + 02	7.05042e + 02	1.33202e + 03	5.35803e + 02	9.79917e + 03	1.85207e + 03	8.98749e + 03	1.63756e + 04	**4.98782e + 02**
	Std	6.38857e + 02	4.42453e + 01	1.87516e + 02	9.16676e + 01	1.03544e + 02	4.17132e + 02	3.46474e + 01	2.35093e + 03	9.02116e + 02	2.64484e + 03	3.79632e + 03	**2.13777e + 01**
CEC2017-F5	Avg	8.48897e + 02	6.22249e + 02	6.81150e + 02	6.43950e + 02	7.71864e + 02	8.62691e + 02	6.17566e + 02	9.07883e + 02	8.47880e + 02	8.99648e + 02	9.99439e + 02	**6.02811e + 02**
	Std	**1.88667e + 01**	3.53393e + 01	3.31437e + 01	4.74467e + 01	3.44558e + 01	6.01543e + 01	3.18978e + 01	2.90502e + 01	4.02519e + 01	4.29298e + 01	2.44975e + 01	2.47492e + 01
CEC2017-F6	Avg	6.75039e + 02	6.13695e + 02	6.40666e + 02	**6.12668e + 02**	6.67499e + 02	6.82050e + 02	6.13666e + 02	6.87730e + 02	6.73726e + 02	6.88680e + 02	6.99825e + 02	6.13263e + 02
	Std	**3.87747e + 00**	7.96372e + 00	9.02815e + 00	4.24209e + 00	7.30314e + 00	1.60768e + 01	5.13036e + 00	7.93370e + 00	9.62301e + 00	6.37154e + 00	5.60835e + 00	7.25786e + 00
CEC2017-F7	Avg	1.23657e + 03	9.33416e + 02	1.01259e + 03	9.25751e + 02	1.32123e + 03	1.31858e + 03	**8.60683e + 02**	1.47889e + 03	1.22521e + 03	1.44657e + 03	2.54320e + 03	8.65634e + 02
	Std	**1.84781e + 01**	4.45813e + 01	5.19967e + 01	6.01164e + 01	6.04930e + 01	7.09502e + 01	3.35566e + 01	6.32483e + 01	7.50515e + 01	1.02763e + 02	9.70126e + 01	3.81489e + 01
CEC2017-F8	Avg	1.09268e + 03	9.16062e + 02	9.42275e + 02	9.04318e + 02	9.89798e + 02	1.06016e + 03	9.07282e + 02	1.16109e + 03	1.07662e + 03	1.16555e + 03	1.24826e + 03	**8.82342e + 02**
	Std	**1.54208e + 01**	2.93342e + 01	2.37721e + 01	2.63094e + 01	2.08597e + 01	4.80333e + 01	3.10739e + 01	2.85414e + 01	2.22614e + 01	3.94035e + 01	2.92644e + 01	1.66093e + 01
CEC2017-F9	Avg	8.67196e + 03	**1.97268e + 03**	3.93400e + 03	2.63516e + 03	8.95363e + 03	1.17168e + 04	2.81084e + 03	1.34215e + 04	7.48978e + 03	1.37239e + 04	2.04320e + 04	2.19061e + 03
	Std	8.82553e + 02	9.47071e + 02	1.27978e + 03	8.90222e + 02	9.58490e + 02	4.11551e + 03	1.30068e + 03	3.23480e + 03	1.48762e + 03	2.46662e + 03	2.41393e + 03	**6.74331e + 02**
CEC2017-F10	Avg	8.62284e + 03	5.70826e + 03	5.17795e + 03	4.83292e + 03	6.22912e + 03	7.50932e + 03	4.78175e + 03	9.68130e + 03	7.95723e + 03	9.44194e + 03	9.20609e + 03	**4.44151e + 03**
	Std	3.88526e + 02	1.09703e + 03	5.96040e + 02	1.04645e + 03	8.42957e + 02	6.57830e + 02	7.01319e + 02	4.14633e + 02	4.25441e + 02	3.57361e + 02	**2.21900e + 02**	9.72092e + 02
CEC2017-F11	Avg	5.13034e + 03	1.44141e + 03	1.51629e + 03	2.22554e + 03	1.58744e + 03	1.09604e + 04	1.34838e + 03	1.40501e + 04	2.83528e + 03	8.70923e + 03	1.28564e + 04	**1.27661e + 03**
	Std	4.52588e + 02	9.03606e + 01	2.81810e + 02	9.94676e + 02	2.32776e + 02	5.24556e + 03	6.62921e + 01	4.00668e + 03	8.39850e + 02	2.90808e + 03	2.77579e + 03	**6.44207e + 01**
CEC2017-F12	Avg	7.03113e + 09	1.15780e + 07	4.10664e + 07	1.31171e + 08	7.81184e + 07	4.62243e + 08	2.11159e + 07	6.05957e + 09	1.72132e + 09	5.90283e + 09	1.03777e + 10	**4.45167e + 06**
	Std	7.79327e + 08	1.29116e + 07	4.70991e + 07	1.45493e + 08	7.82174e + 07	3.33271e + 08	1.68078e + 07	1.95694e + 09	8.78478e + 08	2.40150e + 09	1.72093e + 09	**3.13777e + 06**
CEC2017-F13	Avg	4.31414e + 09	8.13732e + 06	1.28476e + 05	7.37187e + 06	9.51577e + 05	7.32077e + 06	1.50502e + 05	3.45075e + 09	3.76139e + 08	3.64795e + 09	5.63091e + 09	**3.77234e + 04**
	Std	9.07551e + 08	2.16309e + 07	2.32047e + 05	2.82056e + 07	3.86106e + 05	5.18838e + 06	2.22657e + 05	1.47205e + 09	2.02707e + 08	2.05175e + 09	1.42085e + 09	**2.22938e + 04**
CEC2017-F14	Avg	1.93360e + 06	7.67758e + 04	1.33648e + 05	6.63955e + 05	1.40772e + 06	2.13231e + 06	8.53573e + 04	5.13822e + 06	9.49369e + 04	3.04517e + 06	2.84869e + 06	**3.90676e + 04**
	Std	6.12821e + 05	6.97708e + 04	1.57146e + 05	8.67264e + 05	1.79484e + 06	2.11502e + 06	6.70383e + 04	3.44046e + 06	1.25601e + 05	2.20326e + 06	1.42460e + 06	**4.29270e + 04**
CEC2017-F15	Avg	1.33264e + 08	1.54318e + 06	2.15481e + 04	1.41187e + 06	1.36360e + 05	7.54399e + 06	**1.83977e + 04**	2.74471e + 08	2.48083e + 06	2.64158e + 08	7.65253e + 08	2.14530e + 04
	Std	5.70236e + 07	8.14862e + 06	1.30370e + 04	2.36284e + 06	6.32582e + 04	8.25294e + 06	1.26442e + 04	1.67586e + 08	4.92619e + 06	2.13718e + 08	2.99657e + 08	**1.20777e + 04**
CEC2017-F16	Avg	4.67470e + 03	2.89940e + 03	2.81898e + 03	2.69921e + 03	3.70133e + 03	4.51612e + 03	2.74787e + 03	5.01719e + 03	3.94777e + 03	5.05166e + 03	5.27380e + 03	**2.57987e + 03**
	Std	**2.26021e + 02**	4.38316e + 02	3.07934e + 02	4.44447e + 02	4.17387e + 02	8.56111e + 02	2.32360e + 02	4.19383e + 02	3.99029e + 02	3.66055e + 02	3.51051e + 02	3.06396e + 02
CEC2017-F17	Avg	3.10423e + 03	2.38456e + 03	2.32352e + 03	**2.05774e + 03**	2.73058e + 03	2.72810e + 03	2.18215e + 03	3.33161e + 03	2.65298e + 03	3.34081e + 03	3.68145e + 03	2.13599e + 03
	Std	2.01128e + 02	2.70632e + 02	2.09215e + 02	**1.50901e + 02**	2.58900e + 02	2.60164e + 02	1.97499e + 02	2.46103e + 02	2.33268e + 02	3.49467e + 02	2.37454e + 02	2.30470e + 02
CEC2017-F18	Avg	1.19277e + 07	9.68835e + 05	1.54485e + 06	4.04605e + 06	3.68077e + 06	1.60804e + 07	1.24464e + 06	5.67374e + 07	1.77511e + 06	3.32262e + 07	3.92455e + 07	**8.13044e + 05**
	Std	3.65425e + 06	7.98416e + 05	1.33078e + 06	6.38482e + 06	2.89005e + 06	1.69333e + 07	1.42778e + 06	2.80391e + 07	2.30676e + 06	2.67417e + 07	2.31853e + 07	**6.99036e + 05**
CEC2017-F19	Avg	1.28201e + 08	8.56282e + 05	5.53650e + 04	1.46821e + 06	2.04551e + 06	2.63774e + 07	**1.86380e + 04**	3.95695e + 08	8.90558e + 06	4.70818e + 08	1.01041e + 09	2.18757e + 04
	Std	4.10075e + 07	2.77960e + 06	7.51667e + 04	2.83727e + 06	1.64654e + 06	3.22139e + 07	**1.64968e + 04**	2.01765e + 08	1.17846e + 07	5.46801e + 08	4.68118e + 08	2.29818e + 04
CEC2017-F20	Avg	2.82565e + 03	2.51606e + 03	2.65485e + 03	**2.44809e + 03**	2.89208e + 03	2.84879e + 03	2.49898e + 03	3.37431e + 03	2.77814e + 03	3.29520e + 03	3.12666e + 03	2.51740e + 03
	Std	1.06304e + 02	1.65286e + 02	2.06725e + 02	1.60322e + 02	1.97296e + 02	1.78492e + 02	1.63939e + 02	1.91382e + 02	1.91112e + 02	1.66602e + 02	**7.86582e + 01**	1.74227e + 02
CEC2017-F21	Avg	2.62662e + 03	2.43058e + 03	2.45977e + 03	2.41862e + 03	2.58584e + 03	2.63275e + 03	2.40636e + 03	2.69707e + 03	2.59346e + 03	2.68444e + 03	2.75361e + 03	**2.38897e + 03**
	Std	**1.61323e + 01**	3.87700e + 01	3.92745e + 01	5.18677e + 01	6.16382e + 01	4.27005e + 01	2.74609e + 01	3.03243e + 01	3.02389e + 01	4.13638e + 01	2.88252e + 01	2.27227e + 01
CEC2017-F22	Avg	6.00292e + 03	**2.89635e + 03**	6.23062e + 03	5.14378e + 03	7.12652e + 03	8.36760e + 03	5.24716e + 03	9.00058e + 03	6.58236e + 03	8.22503e + 03	9.70938e + 03	3.02887e + 03
	Std	**3.17456e + 02**	1.48572e + 03	1.52797e + 03	2.69097e + 03	1.52813e + 03	1.64426e + 03	1.86828e + 03	1.67832e + 03	2.42104e + 03	1.51516e + 03	7.13821e + 02	1.48135e + 03
CEC2017-F23	Avg	3.29291e + 03	2.91031e + 03	2.83553e + 03	2.78191e + 03	3.33507e + 03	3.10110e + 03	2.79124e + 03	3.38073e + 03	3.06961e + 03	3.32759e + 03	3.38826e + 03	**2.75356e + 03**
	Std	3.48600e + 01	9.80521e + 01	5.30039e + 01	4.43226e + 01	1.40868e + 02	8.58013e + 01	4.09446e + 01	8.96890e + 01	6.33402e + 01	1.16691e + 02	7.15153e + 01	**2.64660e + 01**
CEC2017-F24	Avg	3.55636e + 03	3.08160e + 03	2.98033e + 03	2.97815e + 03	3.48249e + 03	3.23432e + 03	2.93390e + 03	3.57056e + 03	3.21185e + 03	3.55748e + 03	3.62714e + 03	**2.91320e + 03**
	Std	4.89706e + 01	9.73798e + 01	4.86449e + 01	7.02060e + 01	1.54384e + 02	1.11194e + 02	3.31721e + 01	1.13433e + 02	7.01834e + 01	1.25511e + 02	7.04721e + 01	**3.13028e + 01**
CEC2017-F25	Avg	3.57660e + 03	2.92689e + 03	3.01043e + 03	3.03945e + 03	3.00635e + 03	3.19428e + 03	2.92095e + 03	4.85006e + 03	3.42721e + 03	4.96081e + 03	8.72493e + 03	**2.90586e + 03**
	Std	1.13118e + 02	2.92399e + 01	5.68537e + 01	9.70867e + 01	3.96861e + 01	8.95560e + 01	2.73962e + 01	4.42180e + 02	1.87052e + 02	7.16611e + 02	9.54815e + 02	**2.13615e + 01**
CEC2017-F26	Avg	8.99039e + 03	5.39983e + 03	6.30435e + 03	4.85945e + 03	8.16008e + 03	8.60467e + 03	5.08822e + 03	9.67764e + 03	7.40618e + 03	9.86339e + 03	1.11630e + 04	**4.21211e + 03**
	Std	**3.92986e + 02**	1.12184e + 03	9.38609e + 02	5.09459e + 02	1.41840e + 03	8.57195e + 02	5.52827e + 02	6.74124e + 02	1.11932e + 03	8.53699e + 02	6.14480e + 02	1.16005e + 03
CEC2017-F27	Avg	3.96813e + 03	3.31491e + 03	3.32811e + 03	3.27300e + 03	3.60005e + 03	3.54289e + 03	3.25034e + 03	4.10165e + 03	3.46331e + 03	4.01665e + 03	4.11426e + 03	**3.23820e + 03**
	Std	1.25581e + 02	6.34520e + 01	6.56976e + 01	3.15809e + 01	2.01803e + 02	2.02955e + 02	2.06909e + 01	1.94289e + 02	9.45315e + 01	2.00201e + 02	1.44549e + 02	**1.72133e + 01**
CEC2017-F28	Avg	5.14496e + 03	3.42293e + 03	3.46822e + 03	3.51992e + 03	3.51578e + 03	3.87195e + 03	3.28775e + 03	5.96611e + 03	4.25957e + 03	5.84597e + 03	7.71309e + 03	**3.24486e + 03**

Table 6 (*continued*)

Algorithm	Metric	GQPSO	TCSPSO	MELGWO	GWO	HHO	WOA	RIME	CPO	NRBO	SWO	NOA	BBO
	Std	1.02228e + 02	4.19954e + 02	1.39161e + 02	1.65951e + 02	1.19177e + 02	2.12417e + 02	4.80039e + 01	5.52707e + 02	4.22494e + 02	6.66366e + 02	6.69665e + 02	**2.33103e + 01**
CEC2017-F29	Avg	5.52360e + 03	4.01814e + 03	4.43782e + 03	3.96403e + 03	5.09303e + 03	5.38421e + 03	4.09429e + 03	6.20682e + 03	5.07900e + 03	6.21404e + 03	6.46070e + 03	**3.85057e + 03**
	Std	2.34671e + 02	2.66556e + 02	2.84284e + 02	**2.00291e + 02**	6.22510e + 02	5.37078e + 02	2.13720e + 02	5.11147e + 02	3.94574e + 02	6.48281e + 02	4.43897e + 02	2.11276e + 02
CEC2017-F30	Avg	7.50266e + 08	7.38632e + 05	2.48774e + 06	1.65506e + 07	1.03888e + 07	8.91819e + 07	6.97056e + 05	3.99685e + 08	8.69398e + 07	3.91678e + 08	6.43166e + 08	**2.78221e + 05**
	Std	2.22321e + 08	1.42618e + 06	2.10048e + 06	1.80221e + 07	6.81643e + 06	7.53159e + 07	6.44368e + 05	2.67407e + 08	6.39633e + 07	2.17296e + 08	2.34757e + 08	**2.36820e + 05**

descriptions. The maximum iterations and population size were set to 500 and 30, respectively. Each algorithm was run independently 30 times, with the maximum, minimum, mean, and standard deviation of the optimal function values calculated. Furthermore, both Wilcoxon and Friedman statistical tests were employed for comprehensive performance evaluation.

Single diode model

The single-diode model is widely adopted for characterizing the static behavior of solar cells owing to its simplicity and satisfactory accuracy. This equivalent circuit comprises a current source connected in parallel with a diode, a shunt resistor representing leakage current, and a series resistor accounting for power losses. The circuit design of this model is illustrated in Fig. 13.

The output current is formulated in Eq. (7), and the mathematical representation is described in Eq. (8).

$$\begin{cases} I_L = I_{ph} - I_d - I_{sh} \\ I_d = I_{sd} * \left[\exp\left(\frac{q*(V_L+R_S*I_L)}{n*k*T}\right) - 1\right] \\ I_{sh} = \frac{V_L+R_S*I_L}{R_{sh}} \end{cases} \tag{7}$$

$$\begin{cases} f_k(V_L, I_L, x) = I_{ph} - I_{sd} * \left[\exp\left(\frac{q*(V_L+R_S*I_L)}{n*k*T}\right) - 1\right] - \frac{V_L+R_S*I_L}{R_{sh}} - I_L \\ x = \{I_{ph}, I_{sd}, R_S, R_{Sh}, n\} \end{cases} \tag{8}$$

where I_L is the output current of the solar cell, I_{ph} is the represents the total photogenerated current, I_d refers to diode current, and I_{sh} is the shunt leakage current. R_S and R_{sh} correspond to the series and shunt resistances, respectively. V_L designates the output voltage of the cell, I_{sd} stands for the reverse saturation current of the diode. n is the ideality factor of the diode, k is the Boltzmann constant, q equals the electron charge, and T refers to the absolute temperature of the cell in Kelvin.

In Table 13, BBO achieves the first-place Friedman ranking for parameter identification in the Single diode model problem. The Wilcoxon test confirms statistically significant differences (+) between BBO and all other algorithms. Notably, BBO demonstrates optimal performance in maximum, average, and standard deviation metrics, while RIME achieves the best performance in minimum values. Other strong performers include TCSPSO, RIME and NRBO, with the remaining algorithms showing significantly inferior performance compared to BBO.

Double diode model

To characterize current loss resulting from carrier recombination in the depletion region, the double-diode model has been developed. Its circuit configuration consists of two diodes, a current source, and a shunt resistor connected in parallel. The configuration of this equivalent circuit is shown in Fig. 14.

The output current is formulated in Eq. (9), and the mathematical representation is described in Eq. (10)

$$I_L = I_{ph} - I_{ph} - I_{ph} - I_{ph} = I_{ph} - I_{sd1} * \left[\exp\left(\frac{q*(V_L+R_S*I_L)}{n_1*k*T}\right) - 1\right]$$

$$-I_{sd1} * \left[\exp\left(\frac{q*(V_L+R_S*I_L)}{n_2*k*T}\right) - 1\right] - \frac{V_L+R_S*I_L}{R_{sh}} \tag{9}$$

$$\begin{cases} f_k(V_L, I_L, x) = I_{ph} - I_{sd1} * \left[\exp\left(\frac{q*(V_L+R_S*I_L)}{n_1*k*T}\right) - 1\right] - I_{sd1} * \left[\exp\left(\frac{q*(V_L+R_S*I_L)}{n_2*k*T}\right) - 1\right] \\ \qquad - \frac{V_L+R_S*I_L}{R_{sh}} - I_L \\ x = \{I_{ph}, I_{sd1}, I_{sd2}, R_S, R_{Sh}, n_1, n_2\} \end{cases} \tag{10}$$

Table 7
Experimental results of 12 algorithms on the CEC 2017(Dim = 50).

Algorithm	Metric	GQPSO	TCSPSO	MELGWO	GWO	HHO	WOA	RIME	CPO	NRBO	SWO	NOA	BBO
CEC2017-F1	Avg	6.54499e + 10	1.31180e + 09	1.56256e + 10	1.12637e + 10	5.08554e + 09	2.25107e + 10	4.08269e + 07	9.87215e + 10	5.20220e + 10	9.59314e + 10	1.70072e + 11	**2.93051e + 06**
	Std	2.12584e + 09	6.71184e + 08	5.53102e + 09	3.99751e + 09	1.89027e + 09	5.35785e + 09	1.08486e + 07	1.22634e + 10	6.42676e + 09	1.51398e + 10	1.47735e + 10	**2.08733e + 06**
CEC2017-F2	Avg	9.49945e + 71	7.04673e + 53	2.47986e + 62	5.47082e + 62	4.13254e + 65	5.67952e + 80	2.15571e + 43	3.22746e + 79	5.24706e + 65	5.21222e + 79	1.27297e + 80	**3.69383e + 34**
	Std	3.20287e + 72	3.32103e + 54	1.35671e + 63	2.08160e + 63	2.19065e + 66	2.46626e + 81	1.08884e + 44	1.37613e + 80	2.79204e + 66	2.82801e + 80	5.61395e + 80	**1.67671e + 35**
CEC2017-F3	Avg	1.62751e + 05	1.53972e + 05	1.29873e + 05	1.74399e + 05	1.74614e + 05	2.96309e + 05	2.12115e + 05	7.02925e + 05	1.72643e + 05	3.07890e + 05	3.31272e + 05	**1.21541e + 05**
	Std	**1.11472e + 04**	2.72854e + 04	2.38456e + 04	2.77197e + 04	2.00956e + 04	1.00585e + 05	4.73182e + 04	8.81908e + 05	4.51976e + 04	1.21278e + 05	3.91470e + 04	3.14984e + 04
CEC2017-F4	Avg	1.65184e + 04	8.10012e + 02	1.90896e + 03	1.62667e + 03	1.85116e + 03	4.75828e + 03	6.81535e + 02	2.66073e + 04	9.43875e + 03	2.72726e + 04	5.18864e + 04	**6.03825e + 02**
	Std	1.17432e + 03	1.19265e + 02	9.21621e + 02	8.20567e + 02	4.19686e + 02	1.38151e + 03	7.57838e + 01	5.38054e + 03	2.52645e + 03	5.43675e + 03	8.28751e + 03	**4.18864e + 01**
CEC2017-F5	Avg	1.12087e + 03	8.40494e + 02	8.57827e + 02	7.99962e + 02	9.47017e + 02	1.11510e + 03	7.56654e + 02	1.24630e + 03	1.12504e + 03	1.23176e + 03	1.45096e + 03	**7.14886e + 02**
	Std	**2.25542e + 01**	6.46479e + 01	4.54627e + 01	9.45097e + 01	3.43043e + 01	8.87658e + 01	4.85784e + 01	3.73509e + 01	3.92463e + 01	3.07895e + 01	3.58218e + 01	5.21287e + 01
CEC2017-F6	Avg	6.91476e + 02	6.33734e + 02	6.56911e + 02	**6.26188e + 02**	6.81527e + 02	6.97764e + 02	6.31749e + 02	7.03779e + 02	6.92273e + 02	7.06119e + 02	7.21349e + 02	6.32779e + 02
	Std	**4.05103e + 00**	1.17265e + 01	9.54652e + 00	6.71308e + 00	4.58023e + 00	1.30148e + 01	7.18449e + 00	8.25380e + 00	7.03280e + 00	7.53679e + 00	6.39982e + 00	1.02689e + 01
CEC2017-F7	Avg	1.74909e + 03	1.26865e + 03	1.47070e + 03	1.14921e + 03	1.88874e + 03	1.90897e + 03	1.11052e + 03	2.15484e + 03	1.80170e + 03	2.09169e + 03	4.65814e + 03	**1.07521e + 03**
	Std	**3.55031e + 01**	7.41191e + 01	8.73402e + 01	7.72474e + 01	7.69084e + 01	9.70684e + 01	6.54274e + 01	1.04827e + 02	1.09883e + 02	1.00579e + 02	2.19973e + 02	6.79862e + 01
CEC2017-F8	Avg	1.40171e + 03	1.12829e + 03	1.14498e + 03	1.06393e + 03	1.23605e + 03	1.40391e + 03	1.05734e + 03	1.53367e + 03	1.43009e + 03	1.54063e + 03	1.74964e + 03	**1.00989e + 03**
	Std	**1.51032e + 01**	6.28619e + 01	3.91483e + 01	3.73492e + 01	3.39037e + 01	7.91590e + 01	5.14007e + 01	4.87951e + 01	3.68961e + 01	4.93269e + 01	3.88395e + 01	4.36576e + 01
CEC2017-F9	Avg	3.22696e + 04	1.39871e + 04	1.29227e + 04	1.22071e + 04	3.18711e + 04	4.08700e + 04	1.17637e + 04	4.54553e + 04	2.97033e + 04	4.71682e + 04	6.32963e + 04	**6.80571e + 03**
	Std	2.63151e + 03	6.12136e + 03	2.48898e + 03	5.39697e + 03	3.45653e + 03	1.24234e + 04	5.79481e + 03	7.47804e + 03	4.23778e + 03	6.40249e + 03	6.47286e + 03	**1.94125e + 03**
CEC2017-F10	Avg	1.47565e + 04	1.11959e + 04	8.54792e + 03	8.99894e + 03	1.06972e + 04	1.34355e + 04	8.44911e + 03	1.65364e + 04	1.43761e + 04	1.61395e + 04	1.57399e + 04	**7.10851e + 03**
	Std	5.48759e + 02	1.49802e + 03	7.71684e + 02	2.73025e + 03	1.24177e + 03	8.92925e + 02	9.36443e + 02	**4.98089e + 02**	7.04939e + 02	6.53120e + 02	5.30702e + 02	1.02628e + 03
CEC2017-F11	Avg	1.49695e + 04	2.15389e + 03	4.67310e + 03	7.96235e + 03	3.07598e + 03	8.67843e + 03	1.79306e + 03	3.11967e + 04	9.38397e + 03	2.62924e + 04	3.79249e + 04	**1.44887e + 03**
	Std	1.21851e + 03	3.19980e + 02	1.92582e + 03	3.01868e + 03	6.27089e + 02	2.43905e + 03	1.26097e + 02	7.85791e + 03	2.58431e + 03	5.66747e + 03	6.39284e + 03	**9.47038e + 01**
CEC2017-F12	Avg	4.38252e + 10	2.23389e + 08	1.45567e + 09	1.70692e + 09	8.71397e + 08	4.55374e + 09	1.57634e + 08	4.45254e + 10	1.57109e + 10	4.15115e + 10	6.77519e + 10	**2.71552e + 07**
	Std	2.95316e + 09	2.37409e + 08	2.25569e + 09	2.05271e + 09	4.54493e + 08	1.70889e + 09	8.76050e + 07	9.27348e + 09	5.90934e + 09	1.17633e + 10	1.08320e + 10	**1.87995e + 07**
CEC2017-F13	Avg	1.97728e + 10	8.61283e + 07	5.13827e + 07	4.39394e + 08	2.59726e + 07	6.38482e + 08	4.85447e + 05	1.86698e + 10	5.33214e + 09	1.75651e + 10	2.78672e + 10	**8.33150e + 04**
	Std	3.15941e + 09	4.70082e + 08	6.68788e + 07	1.37648e + 09	2.43944e + 07	3.70503e + 08	3.18989e + 05	6.17697e + 09	4.79008e + 09	5.73858e + 09	6.05613e + 09	**4.13938e + 04**
CEC2017-F14	Avg	2.40324e + 07	1.12405e + 06	1.04412e + 06	1.50814e + 06	1.13867e + 07	9.27800e + 06	7.39614e + 05	4.80586e + 07	3.88605e + 06	4.06593e + 07	3.43520e + 07	**3.66227e + 05**
	Std	6.63389e + 06	1.80519e + 06	1.12447e + 06	1.52079e + 06	1.42150e + 07	7.66117e + 06	4.33682e + 05	2.88802e + 07	2.75447e + 06	2.26540e + 07	1.12849e + 07	**2.72566e + 05**
CEC2017-F15	Avg	2.84900e + 09	1.19371e + 07	2.99924e + 06	3.97478e + 07	1.00924e + 07	5.89761e + 07	1.19041e + 05	3.88380e + 09	5.09624e + 08	4.26853e + 09	9.06299e + 09	**3.16801e + 04**
	Std	5.48268e + 08	2.70136e + 07	1.15527e + 07	4.20854e + 07	1.96509e + 07	4.63791e + 07	9.22171e + 04	1.66366e + 09	5.55981e + 08	2.33897e + 09	2.28688e + 09	**1.57907e + 04**
CEC2017-F16	Avg	6.58850e + 03	3.82504e + 03	3.76119e + 03	**3.33521e + 03**	4.91773e + 03	6.48695e + 03	3.75874e + 03	8.03849e + 03	5.86039e + 03	7.57881e + 03	8.87984e + 03	3.39455e + 03
	Std	**2.94392e + 02**	5.37659e + 02	4.58692e + 02	3.73935e + 02	5.21893e + 02	9.50285e + 02	3.99727e + 02	7.56792e + 02	7.33777e + 02	7.99431e + 02	6.67665e + 02	4.48941e + 02
CEC2017-F17	Avg	5.63514e + 03	3.55652e + 03	3.48270e + 03	3.12265e + 03	3.87911e + 03	4.74238e + 03	3.41341e + 03	6.81992e + 03	4.73048e + 03	8.35594e + 03	1.74959e + 04	**3.00740e + 03**
	Std	3.59784e + 02	4.71766e + 02	4.44407e + 02	4.22708e + 02	3.61500e + 02	7.36284e + 02	3.71916e + 02	8.19435e + 02	5.64398e + 02	4.40622e + 03	1.11522e + 04	**2.75422e + 02**
CEC2017-F18	Avg	8.13840e + 07	5.24064e + 06	5.89168e + 06	1.09373e + 07	9.69692e + 06	5.89637e + 07	5.56121e + 06	1.54237e + 08	2.50335e + 07	9.94181e + 07	1.57834e + 08	**2.02622e + 06**
	Std	1.88857e + 07	4.26090e + 06	5.07398e + 06	1.22360e + 07	6.53385e + 06	3.89539e + 07	4.19380e + 06	8.48668e + 07	2.41265e + 07	5.66447e + 07	5.42500e + 07	**1.17166e + 06**
CEC2017-F19	Avg	1.38935e + 09	3.05993e + 05	3.41849e + 05	6.84457e + 06	2.73742e + 06	2.21655e + 07	4.49643e + 05	1.72189e + 09	3.30798e + 08	1.33107e + 09	3.42576e + 09	**7.17014e + 04**
	Std	2.65982e + 08	4.58568e + 05	2.63374e + 05	1.61486e + 07	2.94518e + 06	2.63258e + 07	5.14900e + 05	6.35714e + 08	3.07567e + 08	7.71599e + 08	8.02509e + 08	**3.74561e + 04**
CEC2017-F20	Avg	4.08678e + 03	3.28709e + 03	3.23969e + 03	3.20969e + 03	3.63114e + 03	4.00350e + 03	3.32856e + 03	4.85066e + 03	3.82666e + 03	4.66948e + 03	4.55605e + 03	**3.05444e + 03**
	Std	1.77443e + 02	3.23333e + 02	3.33752e + 02	4.25502e + 02	3.04835e + 02	3.12192e + 02	3.23043e + 02	2.08502e + 02	2.96935e + 02	3.32655e + 02	**1.63590e + 02**	2.87173e + 02
CEC2017-F21	Avg	2.98164e + 03	2.63956e + 03	2.66230e + 03	2.56358e + 03	2.96556e + 03	3.07410e + 03	2.56540e + 03	3.08129e + 03	2.96183e + 03	3.08671e + 03	3.24691e + 03	**2.48996e + 03**
	Std	**2.34151e + 01**	6.63133e + 01	5.81498e + 01	7.96667e + 01	1.04235e + 02	1.10513e + 02	4.70103e + 01	7.82015e + 01	5.91665e + 01	6.26565e + 01	4.75150e + 01	3.69809e + 01
CEC2017-F22	Avg	1.68403e + 04	1.16812e + 04	1.05733e + 04	1.05912e + 04	1.24125e + 04	1.48708e + 04	9.57770e + 03	1.81132e + 04	1.57841e + 04	1.79764e + 04	1.74443e + 04	**8.86800e + 03**
	Std	3.95633e + 02	3.50769e + 03	8.48295e + 02	2.61123e + 03	8.98127e + 02	1.06957e + 03	1.64274e + 03	5.19110e + 02	8.36979e + 02	4.09285e + 02	**3.54273e + 02**	1.52992e + 03
CEC2017-F23	Avg	3.96216e + 03	3.24247e + 03	3.17381e + 03	3.05730e + 03	4.08491e + 03	3.87135e + 03	3.06097e + 03	4.18108e + 03	3.64785e + 03	4.16551e + 03	4.30760e + 03	**2.98321e + 03**
	Std	5.32580e + 01	1.47885e + 02	8.60071e + 01	1.11181e + 02	2.44068e + 02	1.49201e + 02	5.72821e + 01	1.59288e + 02	1.16028e + 02	1.94888e + 02	1.31731e + 02	**4.90355e + 01**
CEC2017-F24	Avg	4.54923e + 03	3.54583e + 03	3.27894e + 03	3.23955e + 03	4.39508e + 03	3.91110e + 03	3.18667e + 03	4.62326e + 03	3.76824e + 03	4.51303e + 03	4.61925e + 03	**3.10866e + 03**
	Std	9.29697e + 01	1.66979e + 02	7.22800e + 01	1.25888e + 02	2.71971e + 02	1.11081e + 02	6.16847e + 01	1.75390e + 02	1.56709e + 02	2.22356e + 02	1.63346e + 02	**5.75890e + 01**
CEC2017-F25	Avg	8.33295e + 03	3.28535e + 03	4.14436e + 03	4.00614e + 03	3.74889e + 03	5.38272e + 03	3.16152e + 03	1.42584e + 04	6.87214e + 03	1.44885e + 04	3.23589e + 04	**3.09165e + 03**
	Std	2.58040e + 02	8.96548e + 01	5.30613e + 02	4.32853e + 02	1.72341e + 02	6.82334e + 02	5.67309e + 01	1.92595e + 03	9.37944e + 02	1.67529e + 03	3.48855e + 03	**3.20108e + 01**
CEC2017-F26	Avg	1.41379e + 04	8.43378e + 03	1.02127e + 04	7.07650e + 03	1.18039e + 04	1.49597e + 04	7.24527e + 03	1.69994e + 04	1.34262e + 04	1.72778e + 04	2.14619e + 04	**6.87580e + 03**
	Std	**3.11522e + 02**	1.48754e + 03	1.72912e + 03	5.96051e + 02	1.06803e + 03	1.71741e + 03	5.93777e + 02	1.01401e + 03	1.44134e + 03	1.15012e + 03	1.31880e + 03	1.47675e + 03
CEC2017-F27	Avg	6.32143e + 03	3.80996e + 03	3.85188e + 03	3.74744e + 03	5.15288e + 03	4.92983e + 03	3.59549e + 03	6.63899e + 03	4.38380e + 03	6.16495e + 03	6.28070e + 03	**3.45993e + 03**
	Std	2.48959e + 02	2.20868e + 02	1.74561e + 02	1.66237e + 02	7.21911e + 02	6.59463e + 02	9.38156e + 01	3.73966e + 02	2.17729e + 02	5.04466e + 02	4.06957e + 02	**7.42492e + 01**
CEC2017-F28	Avg	8.10227e + 03	3.75624e + 03	4.81862e + 03	4.55808e + 03	4.95967e + 03	6.21478e + 03	3.46390e + 03	1.14976e + 04	7.41500e + 03	1.15916e + 04	1.59948e + 04	**3.36909e + 03**

Table 7 (*continued*)

Algorithm	Metric	GQPSO	TCSPSO	MELGWO	GWO	HHO	WOA	RIME	CPO	NRBO	SWO	NOA	BBO
	Std	2.38258e + 02	2.70709e + 02	3.75405e + 02	4.53203e + 02	3.63132e + 02	5.67675e + 02	4.91839e + 01	1.08036e + 03	6.53304e + 02	1.38131e + 03	1.09705e + 03	**3.50709e + 01**
CEC2017-F29	Avg	1.54644e + 04	5.10028e + 03	6.00592e + 03	4.93927e + 03	7.01374e + 03	9.82517e + 03	5.17565e + 03	1.98447e + 04	8.38712e + 03	1.66800e + 04	2.74795e + 04	**4.62226e + 03**
	Std	3.29647e + 03	9.09819e + 02	6.61308e + 02	3.61260e + 02	9.51832e + 02	2.13589e + 03	4.28275e + 02	7.25903e + 03	8.85556e + 02	9.58074e + 03	8.34105e + 03	**3.38550e + 02**
CEC2017-F30	Avg	2.76246e + 09	3.23863e + 07	8.00793e + 07	1.60614e + 08	1.24403e + 08	2.64612e + 08	6.30208e + 07	3.19946e + 09	7.29868e + 08	3.07676e + 09	5.53597e + 09	**2.01165e + 07**
	Std	3.71197e + 08	1.16652e + 08	3.22791e + 07	5.72400e + 07	6.41957e + 07	8.61838e + 07	1.95790e + 07	1.21612e + 09	2.76527e + 08	9.83255e + 08	1.27720e + 09	**3.85175e + 06**

where I_{sd1} and I_{sd1} denote the diffusion and saturation currents, respectively, while n_1 and n_2 represent the ideality factors for the diffusion and recombination diodes, respectively. All other terms retain their previously defined meanings.

In Table 14, BBO secures the top Friedman ranking for parameter identification in the Double diode model problem. The Wilcoxon test demonstrates statistically significant differences (+) between BBO and most competing algorithms. Specifically, BBO achieves optimal performance in both maximum values and standard deviation metrics, while NRBO obtains the best minimum values and RIME shows superior mean values. The Wilcoxon test further indicates no statistically significant differences between BBO and TCSPSO, MELGWO, RIME or NRBO (−), suggesting these algorithms approach BBO's exceptional performance level. GWO exhibits moderate performance, whereas all remaining algorithms demonstrate substantially inferior results compared to BBO.

PV module model

Building upon the single-diode model, extension can be achieved by connecting multiple solar cells in series and/or parallel. The corresponding equivalent circuit configuration is presented in Fig. 15.

The output current is derived from Eq. (11), and the objective function remains consistent with Eq. (8).

$$\frac{I_L}{I_L} = I_L - I_{sd} * \left[\exp\left(\frac{q * \left(\frac{V_L}{N_S} + R_S * \frac{I_L}{N_P} \right)}{n * k * T} \right) - 1 \right] - \frac{\frac{V_L}{N_S} + R_S * \frac{I_L}{N_P}}{R_{sh}} \tag{11}$$

where N_P represents the number of solar cells in parallel, while N_S represents the number of solar cells in series.

In Table 15, BBO achieves the top Friedman ranking for parameter identification in the PV module model. The Wilcoxon test confirms statistically significant differences (+) between BBO and nearly all competing algorithms, while simultaneously demonstrating BBO's optimal performance across all statistical metrics. Notably, the Wilcoxon test reveals no significant difference between TCSPSO and BBO (−), indicating TCSPSO approaches BBO's exceptional performance level. Other strong performers include RIME and NRBO, with MELGWO and GWO showing moderate results. The remaining algorithms exhibit substantially inferior performance compared to BBO.

The application of four engineering optimization problems using the BBO

Complex and highly constrained conditions characterize Engineering Optimization Problems (EOPs), which in turn make algorithmic solutions more difficult. In the process of finding solutions, algorithms must consider both the scope of variables and solution precision, which emphasizes the importance of evaluating the algorithm's ability to solve various engineering design problems. This section demonstrates the strength of the BBO algorithm in solving four classic EOPs: speed reducer weight minimization, three-bar truss design, step-cone pulley optimization, and robot gripper design [59–61]. For all problems, the parameter settings of BBO and its competitors remain consistent with the previous descriptions. The maximum iterations and population size were set to 500 and 30, respectively. Each algorithm was run independently 30 times, with the maximum, minimum, mean, and standard deviation of the optimal function values calculated. Furthermore, both Wilcoxon and Friedman statistical tests were employed for comprehensive performance evaluation.

Table 8
Experimental results of 12 algorithms on the CEC 2017(Dim = 100).

Algorithm	Metric	GQPSO	TCSPSO	MELGWO	GWO	HHO	WOA	RIME	CPO	NRBO	SWO	NOA	BBO
CEC2017-F1	Avg	1.91502e + 11	1.86121e + 10	8.10715e + 10	5.65442e + 10	4.89121e + 10	1.04116e + 11	9.93584e + 08	2.64658e + 11	1.71021e + 11	2.57713e + 11	4.81412e + 11	**8.47926e + 07**
	Std	6.20547e + 09	3.55581e + 09	1.07437e + 10	8.87387e + 09	6.51319e + 09	1.17123e + 10	2.52911e + 08	1.56980e + 10	9.49876e + 09	1.79677e + 10	2.06089e + 10	**2.91580e + 07**
CEC2017-F2	Avg	1.04353e + 158	4.94246e + 133	2.84641e + 144	4.63939e + 139	3.98940e + 154	2.05087e + 172	1.62936e + 125	1.34812e + 172	1.57395e + 160	2.48269e + 176	1.81230e + 177	**6.27711e + 105**
	Std	**6.55350e + 04**	2.41179e + 134	9.23313e + 144	2.47899e + 140	**6.55350e + 04**	**6.55350e + 04**	8.88404e + 125	**6.55350e + 04**	**6.55350e + 04**	**6.55350e + 04**	**6.55350e + 04**	3.35595e + 106
CEC2017-F3	Avg	3.54813e + 05	**3.40459e + 05**	5.17070e + 05	5.29634e + 05	3.45724e + 05	9.32167e + 05	6.94742e + 05	7.64777e + 06	4.07141e + 05	8.79854e + 05	7.62451e + 05	4.65669e + 05
	Std	**1.31068e + 04**	1.63025e + 04	1.30220e + 05	7.68808e + 04	1.49604e + 04	1.46113e + 05	1.03316e + 05	1.65499e + 07	8.30383e + 04	6.26481e + 05	7.59614e + 04	5.98592e + 04
CEC2017-F4	Avg	5.15033e + 04	2.69882e + 03	9.34851e + 03	5.87165e + 03	9.51486e + 03	2.03926e + 04	1.14963e + 03	8.52646e + 04	2.94364e + 04	8.33926e + 04	1.72525e + 05	**8.94113e + 02**
	Std	4.02309e + 03	4.91807e + 02	2.24262e + 03	1.54260e + 03	2.42513e + 03	4.78673e + 03	1.08402e + 02	1.10029e + 04	5.18615e + 03	1.36535e + 04	1.61477e + 04	**8.31851e + 01**
CEC2017-F5	Avg	1.96786e + 03	1.61074e + 03	1.44603e + 03	1.23543e + 03	1.68010e + 03	1.92570e + 03	1.32740e + 03	2.19039e + 03	1.99395e + 03	2.16973e + 03	2.72940e + 03	**1.13868e + 03**
	Std	**3.82185e + 01**	1.12947e + 02	7.35423e + 01	1.11551e + 02	6.15369e + 01	9.87742e + 01	1.28453e + 02	6.26113e + 01	6.08108e + 01	6.35533e + 01	7.72292e + 01	6.38289e + 01
CEC2017-F6	Avg	7.05554e + 02	6.60887e + 02	6.73730e + 02	**6.46188e + 02**	6.91865e + 02	7.08237e + 02	6.55233e + 02	7.17426e + 02	7.04758e + 02	7.15945e + 02	7.40402e + 02	6.48410e + 02
	Std	**2.85594e + 00**	8.81027e + 00	4.84023e + 00	5.58911e + 00	3.68275e + 00	1.02784e + 01	7.58965e + 00	6.40436e + 00	3.61583e + 00	4.89939e + 00	4.72826e + 00	5.60303e + 00
CEC2017-F7	Avg	3.52203e + 03	2.41689e + 03	3.01087e + 03	2.20684e + 03	3.81409e + 03	3.79607e + 03	2.20587e + 03	4.33780e + 03	3.71674e + 03	4.20520e + 03	1.10922e + 04	**1.99623e + 03**
	Std	**8.57965e + 01**	1.35555e + 02	1.73990e + 02	1.45620e + 02	1.06892e + 02	1.27811e + 02	2.22158e + 02	2.42080e + 02	1.87511e + 02	2.25084e + 02	3.71671e + 02	1.68388e + 02
CEC2017-F8	Avg	2.35267e + 03	1.88879e + 03	1.84762e + 03	1.56149e + 03	2.13692e + 03	2.37956e + 03	1.61329e + 03	2.61423e + 03	2.47707e + 03	2.63599e + 03	3.11152e + 03	**1.45437e + 03**
	Std	**3.12913e + 01**	9.57630e + 01	7.69621e + 01	5.15346e + 01	7.65170e + 01	1.19077e + 02	1.17922e + 02	7.47225e + 01	7.96162e + 01	7.88649e + 01	1.04859e + 02	1.10194e + 02
CEC2017-F9	Avg	7.14754e + 04	5.77736e + 04	3.29725e + 04	4.38901e + 04	6.76801e + 04	7.71941e + 04	5.50508e + 04	1.04155e + 05	7.14332e + 04	1.04909e + 05	1.66675e + 05	**2.73236e + 04**
	Std	**3.59519e + 03**	1.05592e + 04	3.84843e + 03	1.20689e + 04	4.13281e + 03	1.94181e + 04	2.08625e + 04	1.21506e + 04	5.62991e + 03	1.39924e + 04	9.50170e + 03	3.76018e + 03
CEC2017-F10	Avg	3.23475e + 04	2.67742e + 04	1.92916e + 04	2.13773e + 04	2.45110e + 04	2.94206e + 04	1.93530e + 04	3.42886e + 04	3.09187e + 04	3.41702e + 04	3.32824e + 04	**1.56920e + 04**
	Std	**5.77606e + 02**	2.58244e + 03	1.19429e + 03	6.11965e + 03	1.55042e + 03	1.75687e + 03	1.40712e + 03	6.67087e + 02	1.16169e + 03	6.07244e + 02	7.04831e + 02	1.18537e + 03
CEC2017-F11	Avg	1.60262e + 05	1.24963e + 05	6.56200e + 04	9.05349e + 04	1.48262e + 05	3.09725e + 05	4.32158e + 04	3.87742e + 05	1.24860e + 05	2.75130e + 05	3.54309e + 05	**1.76782e + 04**
	Std	1.51237e + 04	2.94849e + 04	1.31632e + 04	2.27484e + 04	3.20738e + 04	1.49439e + 05	1.30668e + 04	9.35424e + 04	2.68710e + 04	5.24054e + 04	5.05383e + 04	**5.43152e + 03**
CEC2017-F12	Avg	1.25125e + 11	2.54367e + 09	1.78424e + 10	1.19072e + 10	1.19670e + 10	3.06977e + 10	1.08589e + 09	1.51475e + 11	7.44679e + 10	1.50575e + 11	2.37639e + 11	**3.30477e + 08**
	Std	5.00890e + 09	9.14315e + 08	9.00249e + 09	3.66017e + 09	4.26390e + 09	6.72398e + 09	4.54375e + 08	2.04017e + 10	1.32823e + 10	2.64461e + 10	2.21919e + 10	**1.08473e + 08**
CEC2017-F13	Avg	2.79319e + 10	4.97449e + 07	2.21311e + 09	1.74617e + 09	2.42531e + 08	2.35971e + 09	1.87125e + 06	3.08943e + 10	1.48435e + 10	3.24194e + 10	5.31628e + 10	**1.31272e + 05**
	Std	1.34333e + 09	1.18615e + 08	1.90778e + 09	1.65026e + 09	1.60825e + 08	8.26677e + 08	7.74553e + 05	6.16571e + 09	3.46070e + 09	6.12080e + 09	6.48792e + 09	**7.12271e + 04**
CEC2017-F14	Avg	2.89693e + 07	9.76676e + 06	6.58250e + 06	1.00445e + 07	9.52696e + 06	1.83773e + 07	7.72472e + 06	1.17441e + 08	2.41050e + 07	9.88115e + 07	2.04957e + 08	**3.56605e + 06**
	Std	2.85803e + 06	5.39400e + 06	3.42453e + 06	5.81000e + 06	3.46338e + 06	8.50503e + 06	3.19989e + 06	4.90749e + 07	9.78043e + 06	4.54579e + 07	4.41518e + 07	**1.32413e + 06**
CEC2017-F15	Avg	1.25430e + 10	6.66895e + 06	4.14270e + 08	2.12552e + 08	2.50953e + 07	5.28813e + 08	3.74671e + 05	1.30992e + 10	4.25869e + 09	1.30552e + 10	2.35813e + 10	**5.76705e + 04**
	Std	1.38484e + 09	2.70702e + 07	5.56805e + 08	3.04883e + 08	4.40223e + 07	2.98208e + 08	1.76146e + 05	2.74784e + 09	1.59983e + 09	3.09763e + 09	3.29216e + 09	**1.80580e + 04**
CEC2017-F16	Avg	1.70930e + 04	7.61007e + 03	8.47092e + 03	6.93939e + 03	9.98297e + 03	1.75443e + 04	7.24277e + 03	1.98083e + 04	1.46713e + 04	1.85898e + 04	2.42272e + 04	**5.98150e + 03**
	Std	**5.97818e + 02**	9.62381e + 02	1.01550e + 03	1.12164e + 03	1.01503e + 03	2.85520e + 03	9.06758e + 02	1.82652e + 03	1.40210e + 03	2.13482e + 03	1.94722e + 03	6.67008e + 02
CEC2017-F17	Avg	2.26415e + 05	6.66072e + 03	8.77606e + 03	5.90431e + 03	7.92256e + 03	5.54495e + 04	6.01654e + 03	1.67181e + 06	8.97386e + 04	1.21583e + 06	4.09317e + 06	**5.03183e + 03**
	Std	7.19818e + 04	6.34676e + 02	4.29544e + 03	4.14757e + 03	8.57953e + 02	1.31082e + 05	6.34064e + 02	2.12088e + 06	9.05863e + 04	1.71797e + 06	2.08403e + 06	**4.75287e + 02**
CEC2017-F18	Avg	4.88822e + 07	1.17167e + 07	8.30050e + 06	1.17045e + 07	9.73711e + 06	2.09706e + 07	1.24032e + 07	2.24925e + 08	3.40820e + 07	1.45573e + 08	3.31909e + 08	**3.59187e + 06**
	Std	9.71420e + 06	7.09422e + 06	5.98139e + 06	8.09736e + 06	4.17726e + 06	9.55338e + 06	7.43976e + 06	8.86335e + 07	1.99231e + 07	6.80048e + 07	1.07714e + 08	**2.35596e + 06**
CEC2017-	Avg	1.12050e + 10	5.40670e + 06	2.25454e + 08	2.53232e + 08	4.77791e + 07	4.52911e + 08	2.20457e + 07	1.39589e + 10	4.66502e + 09	1.49566e + 10	2.47226e + 10	**9.86349e + 05**

Table 8 (*continued*)

Algorithm	Metric	GQPSO	TCSPSO	MELGWO	GWO	HHO	WOA	RIME	CPO	NRBO	SWO	NOA	BBO
F19													
	Std	8.96998e + 08	7.93821e + 06	4.31591e + 08	2.85905e + 08	6.34511e + 07	2.90557e + 08	1.18707e + 07	3.20240e + 09	2.37706e + 09	4.85491e + 09	3.04790e + 09	**5.68589e + 05**
CEC2017-F20	Avg	7.63603e + 03	6.55350e + 03	5.53962e + 03	5.36857e + 03	6.01068e + 03	7.14846e + 03	5.77459e + 03	8.70507e + 03	7.27314e + 03	8.68922e + 03	8.33520e + 03	**5.13792e + 03**
	Std	3.30963e + 02	5.87707e + 02	5.00082e + 02	9.43885e + 02	4.93633e + 02	8.75670e + 02	6.15171e + 02	4.82739e + 02	3.56583e + 02	3.34372e + 02	**2.59406e + 02**	4.75807e + 02
CEC2017-F21	Avg	4.13805e + 03	3.50010e + 03	3.44393e + 03	3.09307e + 03	4.37228e + 03	4.48066e + 03	3.19298e + 03	4.54322e + 03	4.16863e + 03	4.50447e + 03	4.84784e + 03	**2.94491e + 03**
	Std	**5.11943e + 01**	1.37929e + 02	1.08171e + 02	1.42562e + 02	1.65613e + 02	2.12754e + 02	9.92510e + 01	1.58528e + 02	1.05770e + 02	1.39524e + 02	8.78643e + 01	7.70649e + 01
CEC2017-F22	Avg	3.45907e + 04	2.92957e + 04	2.28674e + 04	2.26891e + 04	2.76359e + 04	3.20372e + 04	2.21913e + 04	3.75243e + 04	3.34170e + 04	3.62317e + 04	3.57574e + 04	**1.91410e + 04**
	Std	**4.32640e + 02**	5.19285e + 03	1.53025e + 03	4.39243e + 03	1.90292e + 03	1.58431e + 03	1.62600e + 03	5.32898e + 02	9.74600e + 02	9.42504e + 02	6.56299e + 02	1.77130e + 03
CEC2017-F23	Avg	6.86506e + 03	4.50165e + 03	4.01262e + 03	3.74095e + 03	5.98295e + 03	5.27710e + 03	3.72229e + 03	6.65573e + 03	4.98378e + 03	6.48303e + 03	6.64241e + 03	**3.49579e + 03**
	Std	2.23009e + 02	2.50673e + 02	1.89480e + 02	9.77433e + 01	5.12998e + 02	2.27810e + 02	1.31862e + 02	3.69302e + 02	2.02467e + 02	3.12248e + 02	2.16192e + 02	**8.44901e + 01**
CEC2017-F24	Avg	9.53389e + 03	5.63246e + 03	4.74213e + 03	4.48724e + 03	8.38185e + 03	6.83223e + 03	4.23748e + 03	1.03056e + 04	6.16393e + 03	1.00972e + 04	1.07415e + 04	**3.96680e + 03**
	Std	2.57875e + 02	4.94630e + 02	1.81556e + 02	1.43643e + 02	5.38098e + 02	4.06319e + 02	1.79328e + 02	7.85972e + 02	3.80488e + 02	7.10969e + 02	4.69977e + 02	**8.99156e + 01**
CEC2017-F25	Avg	1.75194e + 04	5.74867e + 03	7.81407e + 03	7.11077e + 03	6.84613e + 03	1.08862e + 04	3.92645e + 03	3.01980e + 04	1.51139e + 04	2.79923e + 04	8.49241e + 04	**3.56365e + 03**
	Std	5.84942e + 02	4.57836e + 02	1.48468e + 03	8.95873e + 02	4.97868e + 02	1.02282e + 03	1.11129e + 02	2.81640e + 03	1.60095e + 03	2.54519e + 03	7.76884e + 03	**6.17984e + 01**
CEC2017-F26	Avg	3.74596e + 04	2.11134e + 04	2.50445e + 04	1.75257e + 04	3.11453e + 04	3.86065e + 04	1.61965e + 04	4.96228e + 04	3.62419e + 04	5.09356e + 04	6.41737e + 04	**1.44536e + 04**
	Std	**8.85548e + 02**	4.05150e + 03	3.69245e + 03	1.58174e + 03	1.90738e + 03	3.54705e + 03	2.05886e + 03	3.03999e + 03	3.46136e + 03	4.52260e + 03	4.00901e + 03	4.43832e + 03
CEC2017-F27	Avg	1.07892e + 04	4.24380e + 03	4.62090e + 03	4.22571e + 03	6.85590e + 03	6.13691e + 03	4.03324e + 03	1.22107e + 04	6.35457e + 03	1.14290e + 04	1.19174e + 04	**3.73352e + 03**
	Std	5.89399e + 02	3.61071e + 02	2.59249e + 02	1.79685e + 02	9.34878e + 02	6.27193e + 02	1.11443e + 02	8.34113e + 02	5.52022e + 02	9.64921e + 02	9.02346e + 02	**9.28108e + 01**
CEC2017-F28	Avg	1.93425e + 04	8.05871e + 03	9.60924e + 03	9.58190e + 03	9.30597e + 03	1.45828e + 04	4.20132e + 03	3.15173e + 04	1.99245e + 04	3.40447e + 04	5.26696e + 04	**3.65226e + 03**
	Std	5.92724e + 02	3.66489e + 03	1.11149e + 03	1.48578e + 03	5.91551e + 02	9.76580e + 02	2.86748e + 02	2.63951e + 03	2.03001e + 03	3.44253e + 03	3.51755e + 03	**5.29675e + 01**
CEC2017-F29	Avg	8.38270e + 04	8.96790e + 03	1.25263e + 04	9.48289e + 03	1.31183e + 04	2.01005e + 04	9.65729e + 03	2.18795e + 05	2.94969e + 04	1.55030e + 05	7.77694e + 05	**8.07275e + 03**
	Std	1.71860e + 04	7.31417e + 02	1.78729e + 03	8.49323e + 02	1.26593e + 03	4.50490e + 03	8.99065e + 02	1.28881e + 05	1.25729e + 04	1.29255e + 05	5.07279e + 05	**5.96087e + 02**
CEC2017-F30	Avg	2.65985e + 10	4.52346e + 07	1.72752e + 09	1.11935e + 09	7.38967e + 08	2.97269e + 09	1.72012e + 08	2.48263e + 10	1.20495e + 10	2.59831e + 10	3.84572e + 10	**2.10858e + 07**
	Std	1.63187e + 09	2.56474e + 07	1.33182e + 09	1.17517e + 09	4.11923e + 08	1.38235e + 09	6.56564e + 07	5.32693e + 09	4.15512e + 09	7.38533e + 09	3.58590e + 09	**1.20416e + 07**

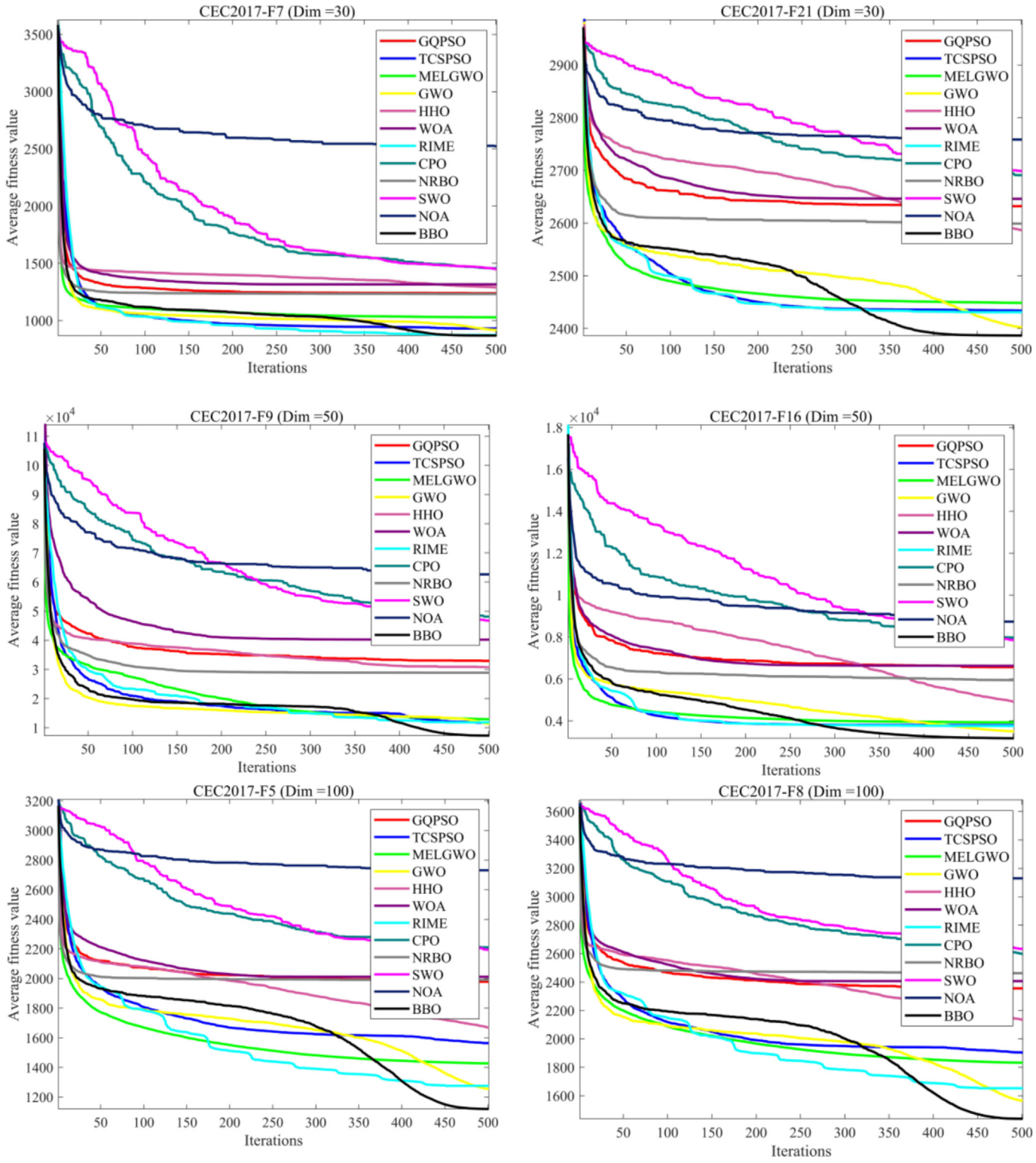

Fig. 7. Comparison of iteration curves of different algorithms on CEC 2017 test suite.

minimization of a speed reducer

This task aims to minimize the total mass of the speed reducer illustrated in Fig. 16. The problem involves seven design variables: face width, gear module, number of teeth, first and second length of shafts between bearings and the lengths between bearings for the first and second shafts. The third variable needs to be constrained to be an integer, and in this problem, there are 11 nonlinear constraints. The task is described mathematically by the formula below:

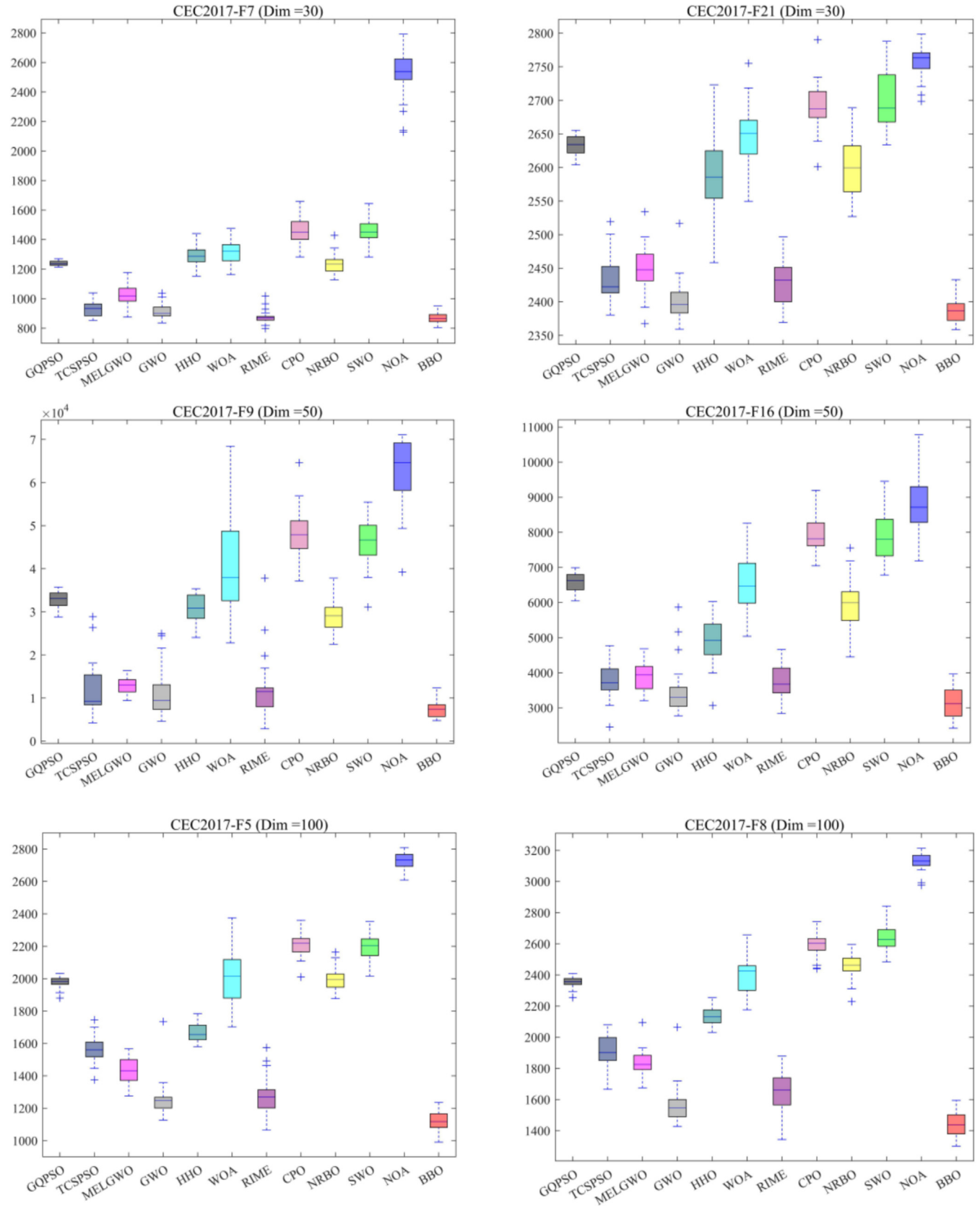

Fig. 8. Comparison of boxplot of different algorithms on CEC 2017 test suite.

Table 9
Wilcoxon signed-rank test on CEC 2022.

BBO vs.	CEC2022 (Dim = 10)	CEC2022 (Dim = 20)
GQPSO	11/1/0	11/1/0
TCSPSO	10/2/0	7/5/0
MELGWO	11/1/0	12/0/0
GWO	12/0/0	6/6/0
HHO	6/3/3	12/0/0
WOA	10/2/0	12/0/0
RIME	10/1/1	7/4/1
CPO	10/1/1	11/1/0
NRBO	11/0/1	12/0/0
SWO	12/0/0	12/0/0
NOA	12/0/0	11/1/0
Overall	**115/11/6**	**113/18/1**

Minimize:

$$f(x) = 0.7854x_1x_2^2(3.333x_3^2 + 14.9334x_3 - 43.0934) - 1.508x_1(x_6^2 + x_7^2) + 7.4777(x_6^3 + x_7^3) + 0.7854(x_4x_6^2 + x_5x_7^2) \quad (12)$$

subject to:

$$g_1(x) = \frac{27}{x_1x_2^2x_3} - 1 \le 0$$
$$g_2(x) = \frac{397.5}{x_1x_2^2x_3^2} - 1 \le 0$$
$$g_3(x) = \frac{1.93x_4^3}{x_2x_3x_6^4} - 1 \le 0 \quad (13)$$
$$g_4(x) = \frac{1.93x_5^3}{x_2x_3x_7^4} - 1 \le 0$$

Table 10
Friedman test on CEC 2022.

Suites	CEC 2022			
Dimensions	10		20	
Algorithms	Ave. Rank	Overall Rank	Ave. Rank	Overall Rank
GQPSO	8.70	9	8.20	9
TCSPSO	3.79	3	3.57	3
MELGWO	3.98	4	4.25	5
GWO	4.69	5	4.23	4
HHO	7.27	7	6.77	6
WOA	7.79	8	7.99	8
RIME	3.34	2	2.94	2
CPO	9.91	11	9.97	10
NRBO	5.98	6	7.07	7
SWO	9.68	10	10.04	11
NOA	10.23	12	10.64	12
BBO	**2.65**	**1**	**2.33**	**1**

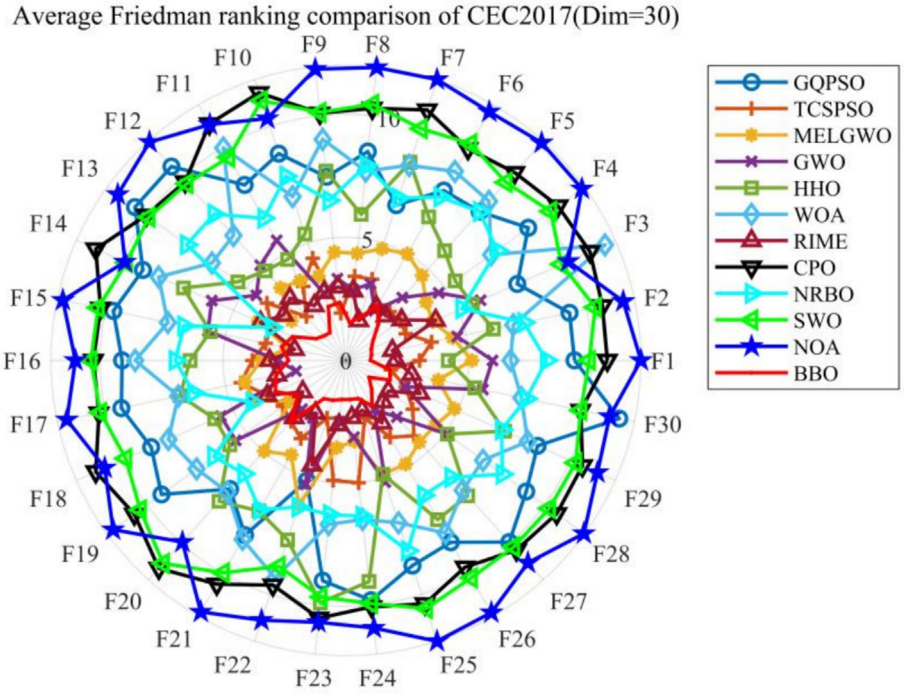

Fig. 9a. Radar chart of average ranking with Friedman test at CEC 2017 (Dim = 30).

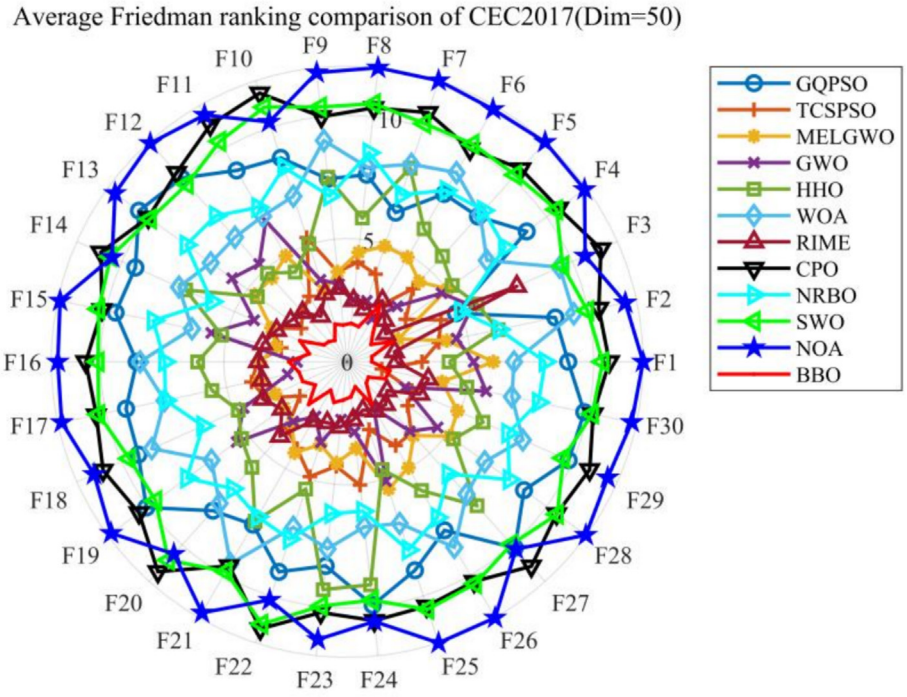

Fig. 9b. Radar chart of average ranking with Friedman test at CEC 2017 (Dim = 50).

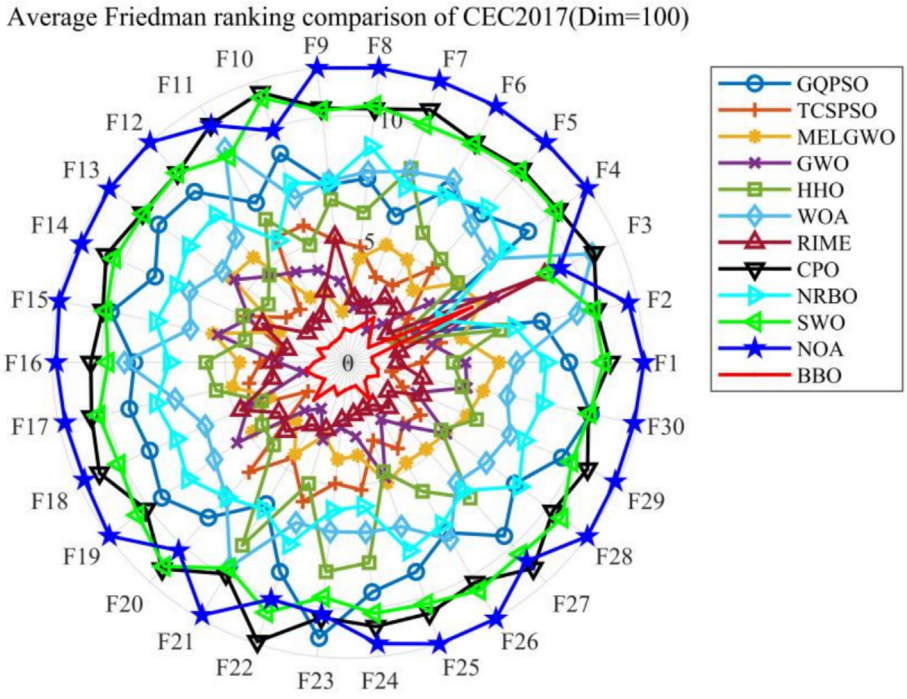

Fig. 9c. Radar chart of average ranking with Friedman test at CEC 2017 (Dim = 100).

$$g_5(x) = \frac{1}{110x_6^3}\sqrt{\left(\frac{745x_4}{x_2x_3}\right)^2 + 16.9\times10^6} - 1 \le 0$$
$$g_6(x) = \frac{1}{85x_7^3}\sqrt{\left(\frac{745x_5}{x_2x_3}\right)^2 + 157.5\times10^6} - 1 \le 0 \quad (14)$$

$$g_7(x) = \frac{x_2x_3}{40} - 1 \le 0$$
$$g_8(x) = \frac{5x_2}{x_1} - 1 \le 0 \quad (15)$$
$$g_9(x) = \frac{x_1}{12x_2} - 1 \le 0$$

Table 11
Experimental results of 12 algorithms on the CEC 2022(Dim = 10).

Algorithm	Metric	GQPSO	TCSPSO	MELGWO	GWO	HHO	WOA	RIME	CPO	NRBO	SWO	NOA	BBO
CEC2022-F1	Avg	4.52249e + 03	4.10792e + 02	3.33734e + 02	3.05783e + 03	1.15243e + 03	3.15000e + 04	3.00672e + 02	1.56054e + 04	1.07655e + 03	1.02574e + 04	1.26929e + 04	**3.00003e + 02**
	Std	8.31032e + 02	1.22872e + 02	1.49544e + 02	2.35172e + 03	4.67892e + 02	1.48281e + 04	5.70160e-01	5.21813e + 03	6.52801e + 02	4.78681e + 03	3.12219e + 03	**2.16612e-03**
CEC2022-F2	Avg	5.93405e + 02	4.11099e + 02	4.14489e + 02	4.33248e + 02	4.60722e + 02	4.84813e + 02	4.16269e + 02	6.73323e + 02	4.63241e + 02	7.13528e + 02	7.66272e + 02	**4.08042e + 02**
	Std	3.44305e + 01	**1.37044e + 01**	2.34995e + 01	2.61539e + 01	6.82031e + 01	8.05810e + 01	2.65289e + 01	1.22441e + 02	6.90537e + 01	1.87696e + 02	1.01979e + 02	1.99745e + 01
CEC2022-F3	Avg	6.38693e + 02	6.00297e + 02	6.09396e + 02	6.01129e + 02	6.43309e + 02	6.37117e + 02	**6.00267e + 02**	6.38789e + 02	6.23981e + 02	6.36954e + 02	6.49955e + 02	6.00367e + 02
	Std	3.38384e + 00	6.58907e-01	6.97079e + 00	1.41062e + 00	1.26044e + 01	1.15097e + 01	**1.91176e-01**	8.15884e + 00	6.06266e + 00	9.07919e + 00	6.17147e + 00	8.22231e-01
CEC2022-F4	Avg	8.42675e + 02	8.21190e + 02	8.16491e + 02	8.17171e + 02	8.27388e + 02	8.32933e + 02	8.24391e + 02	8.66961e + 02	8.32196e + 02	8.71800e + 02	8.71402e + 02	**8.14294e + 02**
	Std	4.45631e + 00	9.27822e + 00	7.63544e + 00	9.35862e + 00	8.12123e + 00	1.27226e + 01	9.88865e + 00	1.08355e + 01	8.24442e + 00	1.12534e + 01	8.43844e + 00	**3.86211e + 00**
CEC2022-F5	Avg	1.12693e + 03	**9.00785e + 02**	9.74806e + 02	9.25845e + 02	1.42068e + 03	1.55046e + 03	9.00949e + 02	1.46269e + 03	1.08511e + 03	1.65202e + 03	1.95698e + 03	9.00977e + 02
	Std	5.85396e + 01	**8.96481e-01**	7.99095e + 01	5.90289e + 01	1.76055e + 02	5.27821e + 02	1.15044e + 00	2.08317e + 02	1.32704e + 02	3.63463e + 02	3.11749e + 02	2.37262e + 00
CEC2022-F6	Avg	4.63553e + 06	6.29705e + 03	3.60654e + 03	5.14721e + 03	6.10643e + 03	5.40770e + 03	3.94154e + 03	2.36092e + 07	3.19273e + 03	2.00909e + 07	3.74000e + 07	**3.03919e + 03**
	Std	3.00121e + 06	2.15365e + 03	1.75675e + 03	2.33470e + 03	4.11632e + 03	3.19375e + 03	2.04587e + 03	1.44811e + 07	1.65566e + 03	2.90504e + 07	2.12610e + 07	**1.39792e + 03**
CEC2022-F7	Avg	2.09710e + 03	**2.01926e + 03**	2.03893e + 03	2.03672e + 03	2.08174e + 03	2.08952e + 03	2.02188e + 03	2.09799e + 03	2.06905e + 03	2.09429e + 03	2.09807e + 03	2.02408e + 03
	Std	1.31332e + 01	**5.77037e + 00**	2.36299e + 01	1.83549e + 01	3.35635e + 01	3.93589e + 01	2.30260e + 01	2.18161e + 01	3.01488e + 01	2.84480e + 01	1.69723e + 01	1.07796e + 01
CEC2022-F8	Avg	2.23578e + 03	2.22754e + 03	2.22680e + 03	2.22578e + 03	2.23688e + 03	2.23541e + 03	2.22061e + 03	2.25070e + 03	2.24655e + 03	2.24502e + 03	2.24824e + 03	**2.22032e + 03**
	Std	**3.43045e + 00**	2.31580e + 01	2.27962e + 01	5.27859e + 00	1.43611e + 01	7.85107e + 00	3.66167e + 00	8.04340e + 00	4.33267e + 01	1.16473e + 01	9.69471e + 00	6.49318e + 00
CEC2022-F9	Avg	2.67486e + 03	2.54254e + 03	2.53349e + 03	2.57779e + 03	2.61726e + 03	2.62959e + 03	2.52929e + 03	2.68324e + 03	2.56077e + 03	2.66498e + 03	2.69036e + 03	**2.52928e + 03**
	Std	1.25865e + 01	3.29535e + 01	1.28484e + 01	3.17113e + 01	4.69935e + 01	5.70134e + 01	2.02961e-03	2.49438e + 01	2.66953e + 01	3.53399e + 01	3.30073e + 01	**5.57235e-05**
CEC2022-F10	Avg	2.56892e + 03	2.54465e + 03	2.59444e + 03	2.55669e + 03	2.58425e + 03	2.68180e + 03	2.55822e + 03	2.57843e + 03	2.57322e + 03	2.57423e + 03	**2.52922e + 03**	2.56458e + 03
	Std	6.62677e + 01	6.95056e + 01	1.30594e + 02	6.02095e + 01	7.63812e + 01	3.09398e + 02	7.25398e + 01	7.90520e + 01	6.87541e + 01	7.53617e + 01	**8.75017e + 00**	5.71952e + 01
CEC2022-F11	Avg	2.88003e + 03	2.79057e + 03	2.71444e + 03	2.81431e + 03	2.84422e + 03	2.83215e + 03	2.72927e + 03	3.01125e + 03	2.85496e + 03	3.07205e + 03	3.05150e + 03	**2.68341e + 03**
	Std	**3.86305e + 01**	1.66912e + 02	1.57002e + 02	1.84850e + 02	1.38601e + 02	1.60159e + 02	1.51096e + 02	2.36026e + 02	1.79984e + 02	2.68720e + 02	6.36753e + 01	1.41665e + 02
CEC2022-F12	Avg	2.95416e + 03	2.88016e + 03	2.86795e + 03	2.86652e + 03	2.91627e + 03	2.90445e + 03	**2.86597e + 03**	2.96410e + 03	2.86967e + 03	2.95302e + 03	2.93302e + 03	2.86682e + 03
	Std	1.12891e + 01	1.83453e + 01	7.66806e + 00	5.90933e + 00	4.17797e + 01	4.54002e + 01	2.67306e + 00	3.63978e + 01	1.27161e + 01	3.72655e + 01	1.84001e + 01	**1.58734e + 00**

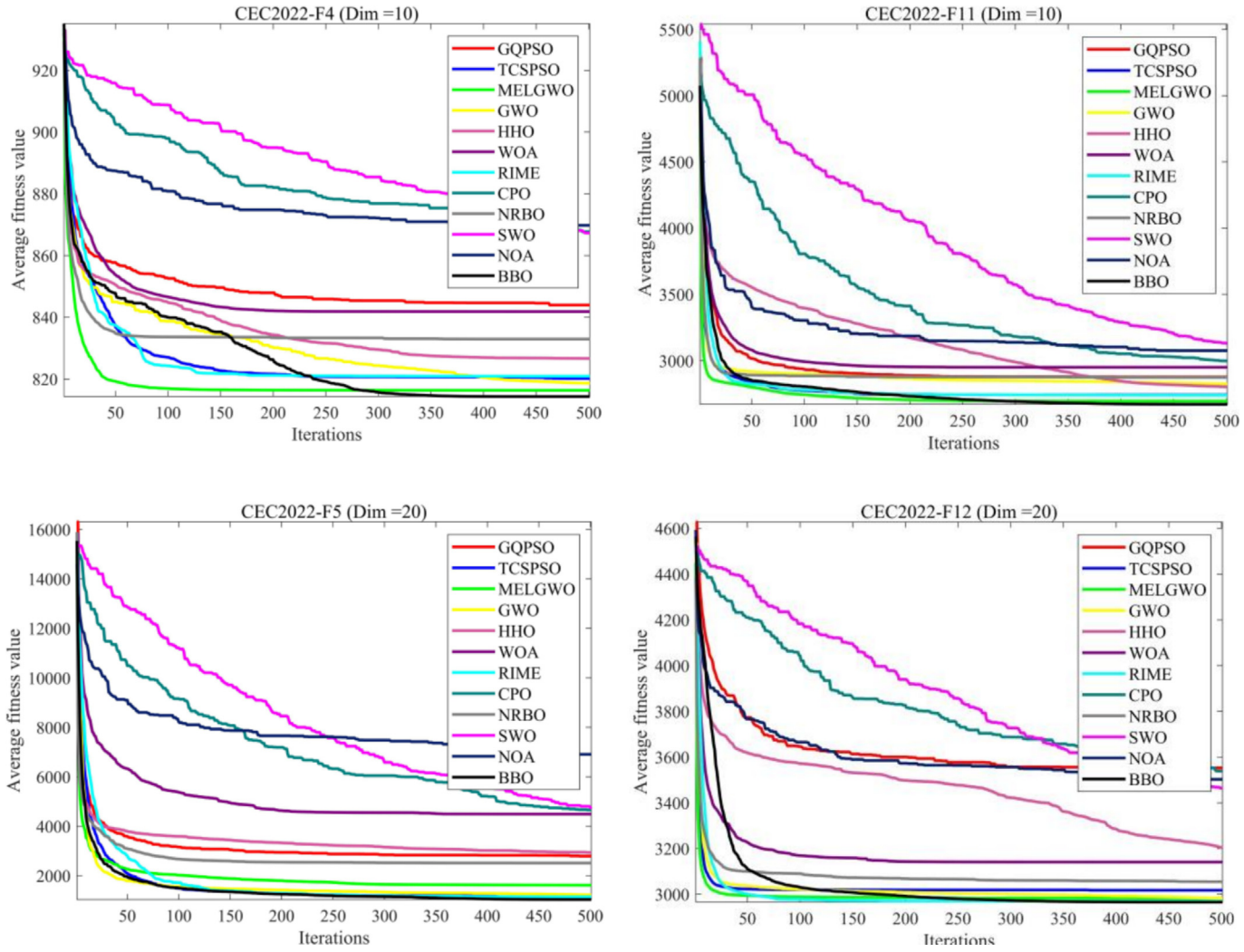

Fig. 10. Comparison of iteration curves of different algorithms on CEC 2022 test suite.

$$g_{10}(x) = \frac{1.5x_6 + 1.9}{x_4} - 1 \le 0 \tag{16}$$

$$g_{11}(x) = \frac{1.1x_7 + 1.9}{x_5} - 1 \le 0 \tag{17}$$

with bounds:

$$2.6 \le x_1 \le 3.6, 0.7 \le x_2 \le 0.8, 17 \le x_3 \le 28$$
$$x_3 \in \mathbb{Z}, \quad 7.3 \le x_4 \le 8.3,$$
$$7.8 \le x_5 \le 8.3, \quad (or 7.3 \le x_5 \le 8.3)$$
$$2.9 \le x_6 \le 3.9, 5.0 \le x_7 \le 5.5$$

In Table 16, BBO secures the top Friedman ranking for parameter identification in the speed reducer problem. The Wilcoxon test demonstrates statistically significant differences (+) between BBO and nearly all competing algorithms. Performance analysis reveals that BBO achieves the best mean values, while MELGWO obtains optimal maximum values and standard deviation, and TCSPSO attains the best minimum values. MELGWO follows closely in second place with minimal performance gap to BBO, and the Wilcoxon test indicates no statistically significant difference between them (−). Other strong performers include RIME, GWO and TCSPSO, ranking third, fourth and fifth respectively. NRBO demonstrates moderate performance, while all remaining algorithms show substantially inferior results compared to BBO.

Three-bar truss design problem

The three-bar truss design problem aims to minimize the structural volume of a statically loaded three-bar truss. This optimization task involves two continuous design variables and must satisfy three nonlinear stress constraints imposed on the individual truss members (σ), with $f(x*) = 263.895843$. Fig. 17 illustrates the schematic configuration of this problem. The complete mathematical formulation is provided below:

Minimize:

$$f(x) = 2\sqrt{2}x_1 + lx_2 \tag{18}$$

subject to:

$$\begin{aligned} g_1(x) &= \frac{\sqrt{2}x_1 + x_2}{\sqrt{2}x_1^2 + 2x_1x_2} P - \sigma \le 0 \\ g_2(x) &= \frac{x_2}{\sqrt{2}x_1^2 + 2x_1x_2} P - \sigma \le 0 \\ g_3(x) &= \frac{1}{\sqrt{2}x_2 + x_1x_2} P - \sigma \le 0 \end{aligned} \tag{19}$$

Table 12
Experimental results of 12 algorithms on the CEC 2022(Dim = 20).

Algorithm	Metric	GQPSO	TCSPSO	MELGWO	GWO	HHO	WOA	RIME	CPO	NRBO	SWO	NOA	BBO
CEC2022-F1	Avg	2.48349e + 04	1.60423e + 04	5.80988e + 03	1.49142e + 04	2.64864e + 04	3.62611e + 04	1.58393e + 03	6.46080e + 04	1.48835e + 04	4.69301e + 04	5.38476e + 04	**4.37729e + 02**
	Std	2.65580e + 03	8.79727e + 03	2.32921e + 03	4.44409e + 03	8.61898e + 03	1.32992e + 04	1.00024e + 03	1.87836e + 04	5.17371e + 03	1.52539e + 04	9.01181e + 03	**1.08553e + 02**
CEC2022-F2	Avg	1.09513e + 03	4.83551e + 02	4.99471e + 02	5.14485e + 02	5.49314e + 02	6.46995e + 02	4.64076e + 02	1.54144e + 03	7.36196e + 02	1.48434e + 03	2.74094e + 03	**4.54025e + 02**
	Std	8.23514e + 01	5.65242e + 01	4.22280e + 01	4.23943e + 01	5.75108e + 01	9.23678e + 01	2.65137e + 01	3.36808e + 02	9.29024e + 01	5.36078e + 02	5.63908e + 02	**1.45323e + 01**
CEC2022-F3	Avg	6.65925e + 02	6.08049e + 02	6.27099e + 02	6.06560e + 02	6.64610e + 02	6.70824e + 02	6.06988e + 02	6.70671e + 02	6.60243e + 02	6.72071e + 02	6.86918e + 02	**6.06287e + 02**
	Std	**3.91953e + 00**	7.00010e + 00	1.02624e + 01	4.03348e + 00	7.09185e + 00	1.22400e + 01	5.32329e + 00	1.00662e + 01	1.00082e + 01	9.50288e + 00	6.47476e + 00	6.55141e + 00
CEC2022-F4	Avg	9.51396e + 02	8.66974e + 02	8.64045e + 02	8.57979e + 02	8.83271e + 02	9.37526e + 02	8.67683e + 02	9.97823e + 02	9.39565e + 02	9.90205e + 02	1.01959e + 03	**8.45804e + 02**
	Std	**1.10433e + 01**	2.08674e + 01	1.87036e + 01	2.42919e + 01	1.21208e + 01	3.68022e + 01	2.28002e + 01	2.18770e + 01	1.94134e + 01	2.18419e + 01	1.58513e + 01	1.42501e + 01
CEC2022-F5	Avg	2.85439e + 03	1.07657e + 03	1.77282e + 03	1.29354e + 03	2.89731e + 03	4.66363e + 03	1.37297e + 03	4.39683e + 03	2.45809e + 03	4.98283e + 03	6.77917e + 03	**1.06125e + 03**
	Std	2.22559e + 02	**1.57313e + 02**	4.04843e + 02	3.54244e + 02	3.48814e + 02	1.85243e + 03	7.31398e + 02	8.34417e + 02	4.38003e + 02	1.15147e + 03	8.66173e + 02	2.20812e + 02
CEC2022-F6	Avg	2.08091e + 08	1.09746e + 04	6.77130e + 03	1.77846e + 06	2.17941e + 05	5.91060e + 06	1.49798e + 04	7.71197e + 08	2.87652e + 07	6.38258e + 08	1.60171e + 09	**4.20160e + 03**
	Std	8.23074e + 07	8.49979e + 03	5.77990e + 03	3.53985e + 06	1.13273e + 05	8.70210e + 06	9.94389e + 03	4.01346e + 08	2.15704e + 07	4.19756e + 08	5.37840e + 08	**2.97233e + 03**
CEC2022-F7	Avg	2.19228e + 03	**2.07499e + 03**	2.14084e + 03	2.10556e + 03	2.19810e + 03	2.26371e + 03	2.08928e + 03	2.28134e + 03	2.17520e + 03	2.26007e + 03	2.23171e + 03	2.08552e + 03
	Std	**1.80844e + 01**	3.77557e + 01	5.15389e + 01	5.69861e + 01	6.68751e + 01	7.20432e + 01	5.29982e + 01	7.20532e + 01	4.60199e + 01	6.54129e + 01	4.43994e + 01	4.48948e + 01
CEC2022-F8	Avg	2.27681e + 03	2.27955e + 03	2.28347e + 03	2.25693e + 03	2.31410e + 03	2.31730e + 03	**2.25287e + 03**	2.44460e + 03	2.29960e + 03	2.47732e + 03	2.50153e + 03	2.25996e + 03
	Std	**2.69780e + 01**	5.91419e + 01	1.04572e + 02	4.87411e + 01	9.74512e + 01	7.61529e + 01	4.54348e + 01	1.03064e + 02	6.84569e + 01	1.37284e + 02	8.15748e + 01	5.47807e + 01
CEC2022-F9	Avg	2.79175e + 03	2.49390e + 03	2.49690e + 03	2.52281e + 03	2.55244e + 03	2.59068e + 03	2.48158e + 03	2.86061e + 03	2.60971e + 03	2.81597e + 03	2.96670e + 03	**2.48117e + 03**
	Std	5.32385e + 01	1.87580e + 01	1.12332e + 01	2.47612e + 01	3.72723e + 01	5.00638e + 01	6.12839e-01	1.07186e + 02	5.34842e + 01	1.17717e + 02	1.03240e + 02	**2.87595e-01**
CEC2022-F10	Avg	2.87735e + 03	3.20525e + 03	3.89071e + 03	3.32514e + 03	4.56858e + 03	5.19379e + 03	**2.81151e + 03**	3.66193e + 03	4.97030e + 03	5.23226e + 03	3.02672e + 03	3.26486e + 03
	Std	5.14519e + 02	6.36760e + 02	7.41068e + 02	9.02726e + 02	7.03690e + 02	1.15655e + 03	3.13997e + 02	1.70092e + 03	1.64596e + 03	1.81846e + 03	**3.12428e + 02**	5.53276e + 02
CEC2022-F11	Avg	6.74427e + 03	3.01770e + 03	3.10175e + 03	3.69981e + 03	3.43613e + 03	3.98120e + 03	2.91921e + 03	6.96505e + 03	4.83530e + 03	7.20289e + 03	8.37893e + 03	**2.91554e + 03**
	Std	1.88441e + 02	2.64946e + 02	2.79590e + 02	5.04521e + 02	5.90336e + 02	5.98142e + 02	9.13575e + 01	6.30210e + 02	7.67445e + 02	9.42138e + 02	7.42151e + 02	**3.38247e + 01**
CEC2022-F12	Avg	3.57501e + 03	3.00921e + 03	2.99399e + 03	2.98320e + 03	3.18833e + 03	3.07398e + 03	**2.96940e + 03**	3.56953e + 03	3.02524e + 03	3.50554e + 03	3.51329e + 03	2.97296e + 03
	Std	8.34885e + 01	3.88972e + 01	4.31019e + 01	3.67131e + 01	1.49852e + 02	7.72061e + 01	**2.33144e + 01**	9.44324e + 01	5.37387e + 01	1.54303e + 02	7.08894e + 01	2.46277e + 01

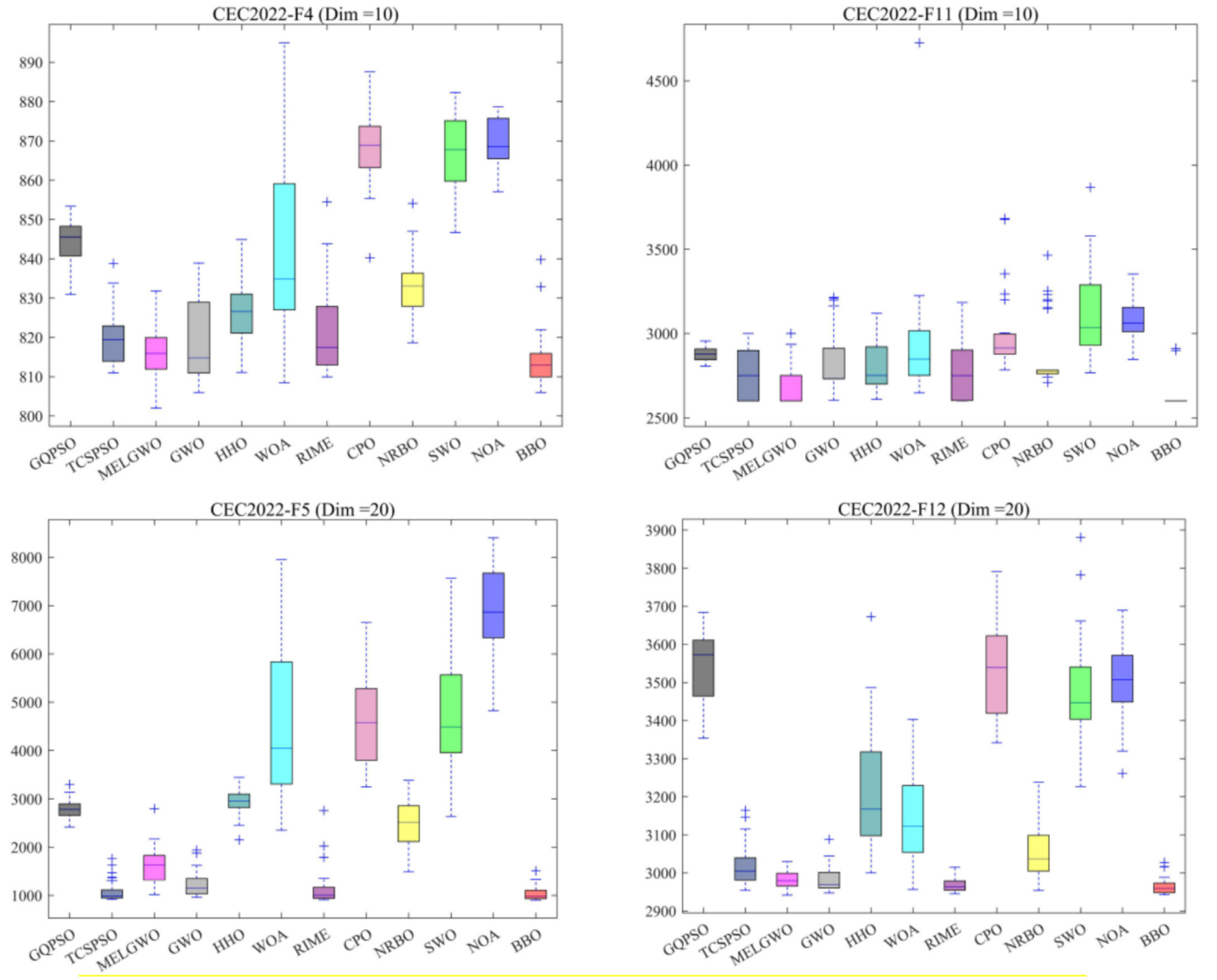

Fig. 11. Comparison of boxplot of different algorithms on CEC 2022 test suite.

where:

$l = 100cm, P = 2kN/cm^2, \sigma = 2kN/cm^2$

with bounds:

$0 \le x_1, x_2 \le l$

In Table 17, BBO achieves the top Friedman ranking for the three-bar truss problem, with Wilcoxon test results showing statistically significant differences (+) between BBO and nearly all comparison algorithms. The performance evaluation demonstrates that BBO attains optimal maximum values, mean values, and standard deviation, while NRBO achieves the best minimum values. The Wilcoxon test reveals no statistically significant differences between BBO and TCSPSO, MELGWO, and NRBO (−), which rank second, third, and fourth respectively – indicating these algorithms approach BBO's exceptional performance level. All remaining algorithms exhibit substantially inferior performance compared to BBO.

Step-cone pulley problem

Fig. 18 depicts the schematic layout of this problem. The objective is to minimize the total weight of a four-step cone pulley by optimizing five design variables: four diameters corresponding to each pulley step and one shared width. Eleven nonlinear constraints are imposed to guarantee a transmitted power of at least 0.75 horsepower. The mathematical formulation is provided below:

Minimize:

$$f\left(\bar{x}\right) = \rho\omega\left[d_1^2\left\{11 + \left(\frac{N_1}{N}\right)^2\right\} + d_2^2\left\{1 + \left(\frac{N_2}{N}\right)^2\right\} + d_3^2\left\{1 + \left(\frac{N_3}{N}\right)^2\right\} + d_4^2\left\{1 + \left(\frac{N_4}{N}\right)^2\right\}\right] \tag{20}$$

subject to:

$$\begin{aligned} h_1\left(\bar{x}\right) &= C_1 - C_2 = 0, \\ h_2\left(\bar{x}\right) &= C_1 - C_3 = 0, \\ h_3\left(\bar{x}\right) &= C_1 - C_4 = 0, \\ g_{i=1,2,3.4}\left(\bar{x}\right) &= -R_i \le 2, \\ g_{i=1,2,3.4}\left(\bar{x}\right) &= (0.75 \times 745.6998) - P_i \le 0 \end{aligned} \tag{21}$$

where:

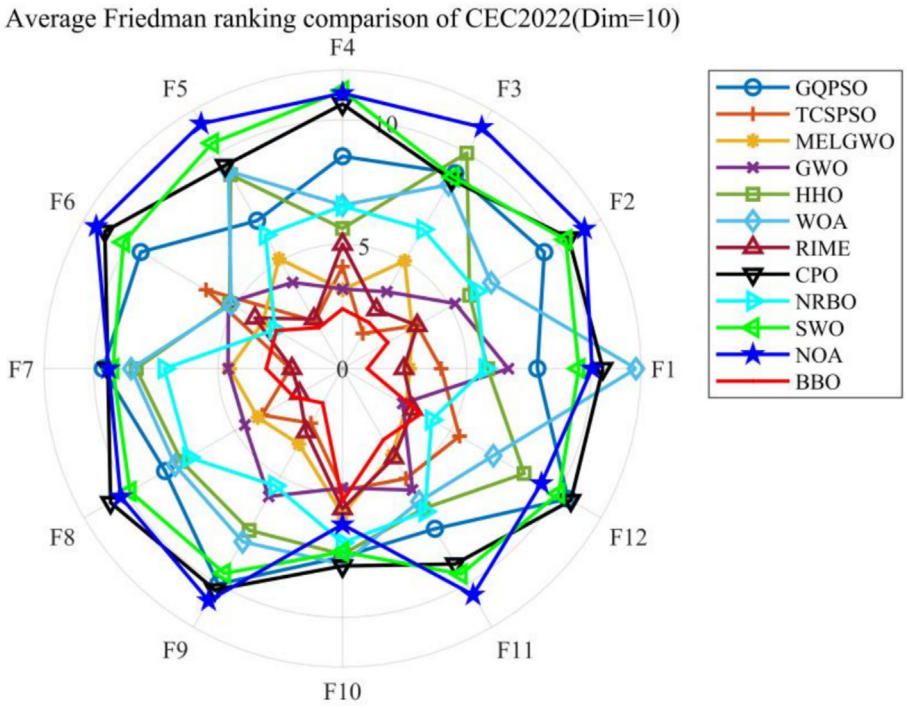

Fig. 12a. Radar chart of average ranking with Friedman test at CEC 2022 (Dim = 10).

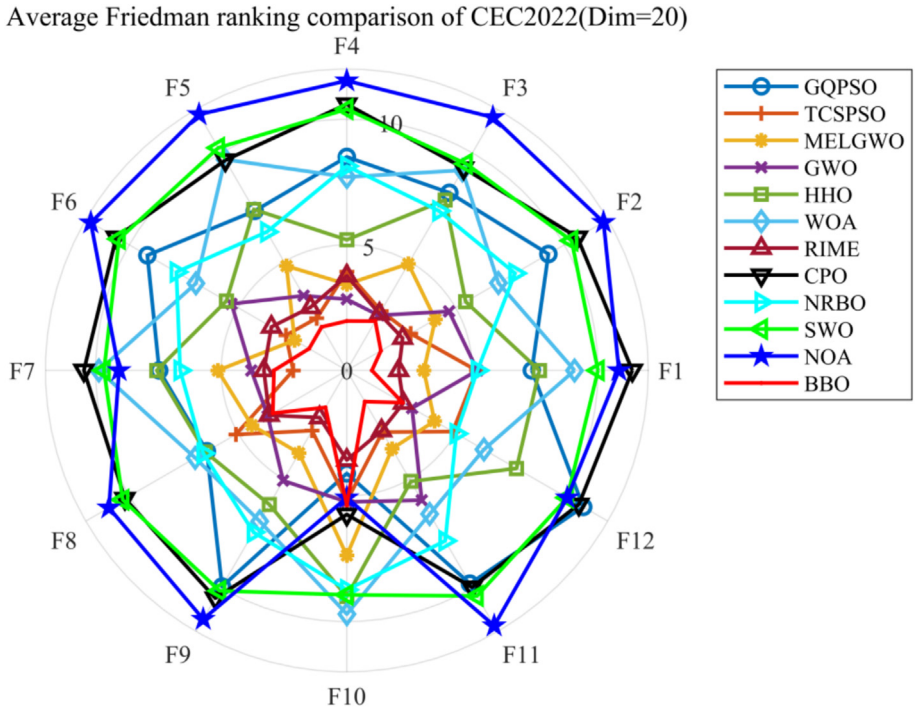

Fig. 12b. Radar chart of average ranking with Friedman test at CEC 2022 (Dim = 20).

$$C_i = \frac{\pi d_i}{2}\left(1+\frac{N_i}{N}\right)+\frac{\left(\frac{N_i}{N}-1\right)^2}{4a}+2a, i=(1,2,3,4),$$
$$R_i = exp\left(\mu\left\{\pi - 2sin^{-1}\left\{\left(\frac{N_i}{N}-1\right)\frac{d_i}{2a}\right\}\right\}\right), i=(1,2,3,4),$$
$$P_i = st\omega(1-R_i)\frac{\pi d_i N_i}{60}, i=(1,2,3,4),$$
$$t=8mm, s=1.75MPa, \mu=0.35, \rho=7200kg/m^3, a=3mm. \quad (22)$$

In Table 18, BBO achieves the top Friedman ranking for the step-cone pulley problem, with Wilcoxon test results demonstrating statistically significant differences (+) between BBO and all com-

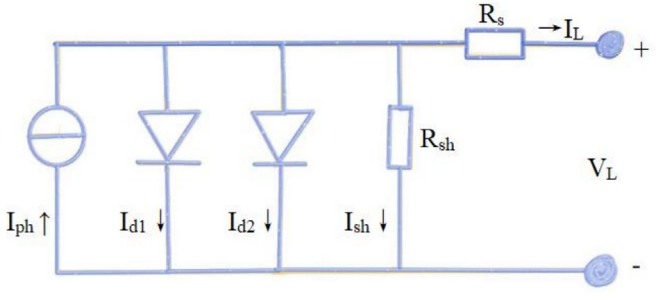

Fig. 13. Single diode model circuit.

Table 13
Results comparison for the single diode model.

Algorithm	Max	Min	Mean	Std	Wilcoxon	Friedman Value
GQPSO	0.210653906	0.018187555	0.067824742	0.040515134	(+)	10.73
TCSPSO	0.046013568	0.001073018	0.005688997	0.011963342	(+)	3.77
MELGWO	0.00861953	0.001011892	0.002786465	0.001916513	(+)	3.90
GWO	0.045711945	0.001640101	0.01084071	0.013660285	(+)	6.07
HHO	0.156554366	0.002069061	0.027792503	0.031567481	(+)	8.13
WOA	0.222868622	0.001365344	0.026414429	0.0427977	(+)	7.40
RIME	0.006279325	**0.000991596**	0.00247076	0.00155614	(+)	3.43
CPO	0.150452496	0.016834852	0.069859744	0.033952944	(+)	11.17
NRBO	0.004374814	0.001096863	0.002193057	0.001016971	(+)	3.20
SWO	0.109758764	0.00730553	0.030524301	0.020903662	(+)	8.77
NOA	0.065044384	0.009919834	0.033439649	0.012192687	(+)	9.13
BBO	**0.002281207**	0.001029431	**0.001573699**	**0.000371476**	/	**2.30**

peting algorithms. Additionally, BBO exhibits optimal performance across all statistical metrics. Other strong performers include TCSPSO, MELGWO and NRBO, ranking second, third and fifth respectively. WOA, RIME and HHO show moderate performance, while the remaining algorithms demonstrate substantially inferior results compared to BBO.

Robot gripper problem

The robot gripper optimization seeks to minimize the variation between the maximum and minimum gripping forces. This is achieved by adjusting the gripper's end-position displacements. As illustrated in Fig. 19, the design incorporates six variables: linkage dimensions a, b, and c, vertical offsets e and f, horizontal distance l, and angle δ. The mathematical formulation is presented below:

Consider:

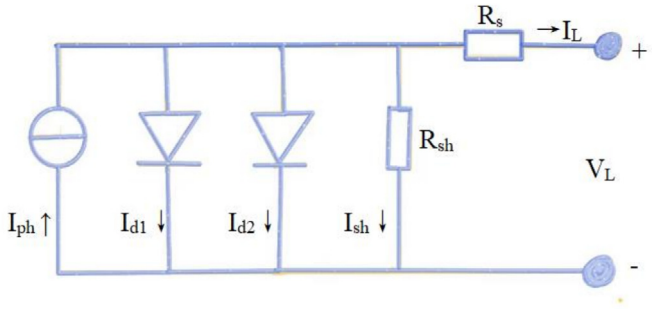

Fig. 14. Double diode model circuit.

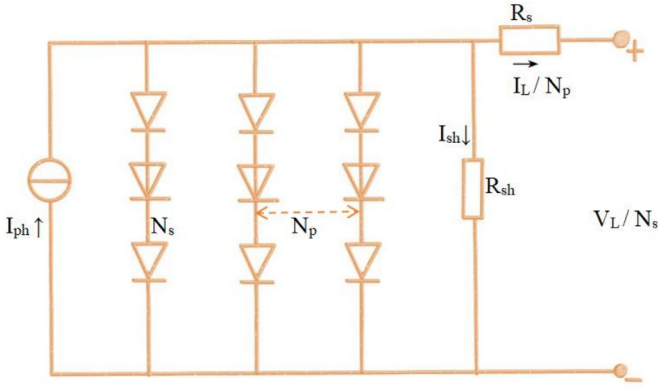

Fig. 15. PV module model circuit.

$$x = [x_1, x_2, x_3, x_4, x_5, x_6, x_7] = [a, b, c, e, f, l, \delta] \tag{23}$$

Minimize:

$$f(x) = -min(z)F_k(x,z) + max(z)F_k(x,z) \tag{24}$$

subject to:

$$\begin{aligned} g_1(x) &= -Y_{min} + y((x), Z_{max}) \le 0 \\ g_2(x) &= -y((x), Z_{max}) \le 0 \\ g_3(x) &= Y_{max} - y((x), 0) \le 0 \\ g_4(x) &= y((x), 0) - Y_G \le 0 \\ g_5(x) &= l^2 + e^2 - (a+b)^2 \le 0 \\ g_6(x) &= b^2 - (a-e)^2 - (l - Z_{max})^2 \le 0 \\ g_7(x) &= Z_{max} - l \le 0 \end{aligned} \tag{25}$$

where:

Table 14
Results comparison for the double diode model.

Algorithm	Max	Min	Mean	Std	Wilcoxon	Friedman Value
GQPSO	0.171008839	0.016136737	0.078498794	0.0362904	(+)	11.17
TCSPSO	0.03948799	0.000984854	0.004383667	0.008820034	(−)	3.37
MELGWO	0.037408625	0.001068051	0.004114167	0.006609122	(−)	3.47
GWO	0.044453426	0.001648816	0.009723878	0.011447052	(+)	5.63
HHO	0.292999598	0.001765425	0.037778689	0.056697176	(+)	7.80
WOA	0.085907165	0.001829584	0.024370834	0.020533357	(+)	7.27
RIME	0.004089729	0.001100021	**0.002294516**	0.000801963	(−)	3.43
CPO	0.153958393	0.01942644	0.064669484	0.031631328	(+)	10.73
NRBO	0.010397542	**0.001005014**	0.003719909	0.002593021	(−)	4.17
SWO	0.083316627	0.007468973	0.032567784	0.020679666	(+)	8.70
NOA	0.065825236	0.016642221	0.03532191	0.012641476	(+)	9.13
BBO	**0.00373982**	0.00136743	0.002311933	**0.000614994**	/	**3.13**

Table 15
Results comparison for the PV module model.

Algorithm	Max	Min	Mean	Std	Wilcoxon	Friedman Value
GQPSO	0.274524455	0.039303809	0.11190439	0.041637256	(+)	10.07
TCSPSO	0.274250778	0.002451097	0.014336295	0.05075383	(−)	2.70
MELGWO	0.274250799	0.002602428	0.021054837	0.068828774	(+)	4.43
GWO	0.274323637	0.002618312	0.015053012	0.050079349	(+)	5.17
HHO	0.297838657	0.003605249	0.108586509	0.097024274	(+)	8.93
WOA	0.276464595	0.00256929	0.123596718	0.127787352	(+)	8.47
RIME	0.274390019	0.002470785	0.01264857	0.049495764	(+)	3.70
CPO	4.546484277	0.024415198	0.409390409	1.044285072	(+)	10.40
NRBO	0.017393175	0.002438122	0.00558803	0.004447007	(+)	4.23
SWO	0.328783764	0.021726428	0.095307585	0.06495935	(+)	9.17
NOA	0.11244788	0.010672912	0.071922101	0.027730886	(+)	8.59
BBO	**0.00351469**	**0.002437562**	**0.00262759**	**0.000204843**	/	**2.23**

Table 16
Comparison results for optimizing a speed reducer for minimum weight.

Algorithm	Max	Min	Mean	Std	Wilcoxon	Friedman Value
GQPSO	1.53186E + 15	2.7988E + 12	2.31478E + 14	2.7491E + 14	(+)	12.00
TCSPSO	3202.582182	**2994.424466**	3047.260587	55.71885432	(+)	4.80
MELGWO	**2999.980765**	2994.834111	2996.512169	**1.499027006**	(−)	2.00
GWO	3025.743866	3002.390633	3011.885211	5.637153673	(+)	4.30
HHO	5388.402509	2997.984549	3825.129219	816.8305644	(+)	8.47
WOA	5690.973631	3030.801248	3386.810935	549.0672889	(+)	7.80
RIME	3007.007721	2995.195376	2998.757468	3.30353079	(+)	2.63
CPO	2.15137E + 13	3257.944592	1.6954E + 12	4.24562E + 12	(+)	10.40
NRBO	3188.504044	3005.064475	3084.019582	56.81551805	(+)	6.10
SWO	1.81364E + 13	3117.139965	6.34213E + 11	3.30848E + 12	(+)	9.20
NOA	3882.613893	3115.447845	3367.520073	202.0316413	(+)	8.40
BBO	3000.225491	2994.425922	**2996.324169**	1.825112367	/	**1.90**

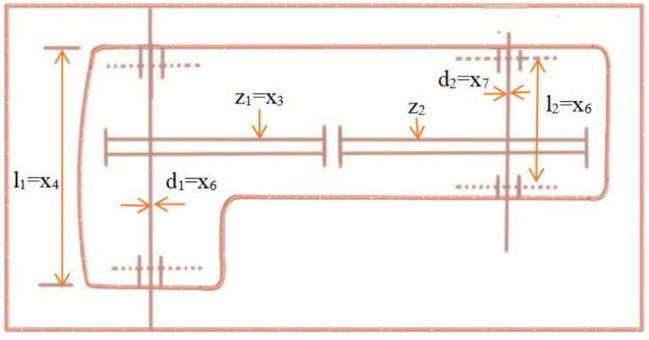

Fig. 16. Schematic view of the speed reducer design.

$$\text{`a} = cos_{-1}\left(\frac{a^2+g^2-b^2}{2ag}\right)+\phi, g=\sqrt{e^2+(z-l)^2}, \beta = cos_{-1}\left(\frac{b^2+g^2-a^2}{2ag}\right)-\phi, \phi = tan_{-1}\left(\frac{e}{l-z}\right), y(x,z) = 2(f+e+csin(\beta+\delta)), F_k = \frac{Pbsin(\alpha+\beta)}{2ccos(\alpha)}, Y_{min}=50, Y_{max}=100, Y_G = 150, Z_{max}=100, P=100. \quad (26)$$

parameters range:

$$0 \le e \le 50, 100 \le c \le 200, 10 \le f, a, b \le 150, 1 \le \delta \le 3.14, 100 \le l \le 300$$

In Table 19, BBO ranks second in the Friedman test for the problem of Robot gripper. However, the Wilcoxon test indicates no statistically significant difference between BBO and the top-ranked MELGWO, demonstrating BBO's equally exceptional performance.

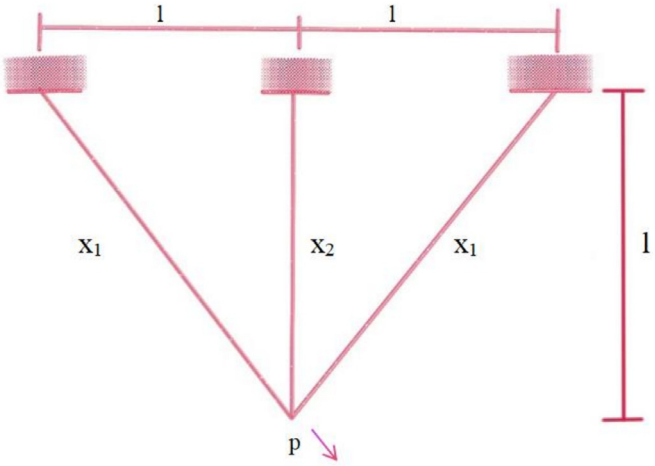

Fig. 17. Schematic view of the three-bar truss design problem.

Similarly, TCSPSO and GWO (ranking third and fourth respectively) show no significant difference from BBO, with performance levels closely trailing BBO's. Detailed performance analysis reveals MELGWO achieves optimal maximum values, mean values and standard deviation, while TCSPSO attains the best minimum values – with BBO's results being highly competitive with these leading algorithms. All remaining algorithms demonstrate substantially inferior performance compared to BBO.

Conclusion

This study proposes the BBO, a novel MA inspired by beavers' self-organizing dam-building behavior. The key findings are summarized as follows:

Table 17
Comparison results for three-bar truss problem.

Algorithm	Max	Min	Mean	Std	Wilcoxon	Friedman Value
GQPSO	266.0936235	263.9195955	264.6233827	0.575894606	(+)	9.17
TCSPSO	263.9063688	263.8958458	263.8970536	0.002005549	(−)	2.53
MELGWO	263.9049502	263.8958435	263.8975746	0.002409868	(−)	2.83
GWO	263.9433782	263.8968164	263.9051372	0.009271922	(+)	4.83
HHO	264.8843909	263.9024453	264.1390537	0.226825951	(+)	7.37
WOA	282.8427125	263.8978626	265.8964633	3.819832618	(+)	9.33
RIME	273.2840157	263.8959352	265.430428	2.407908474	(+)	8.63
CPO	266.6406859	263.9412777	265.2511056	0.802971277	(+)	10.53
NRBO	263.9812009	**263.8958434**	263.9031351	0.017554365	(−)	3.03
SWO	266.7527907	263.904441	264.8432086	0.792581631	(+)	9.53
NOA	264.8937337	263.8964244	264.226835	0.237710542	(+)	7.87
BBO	**263.8991253**	263.8958442	**263.8966627**	**0.000970353**	/	**2.33**

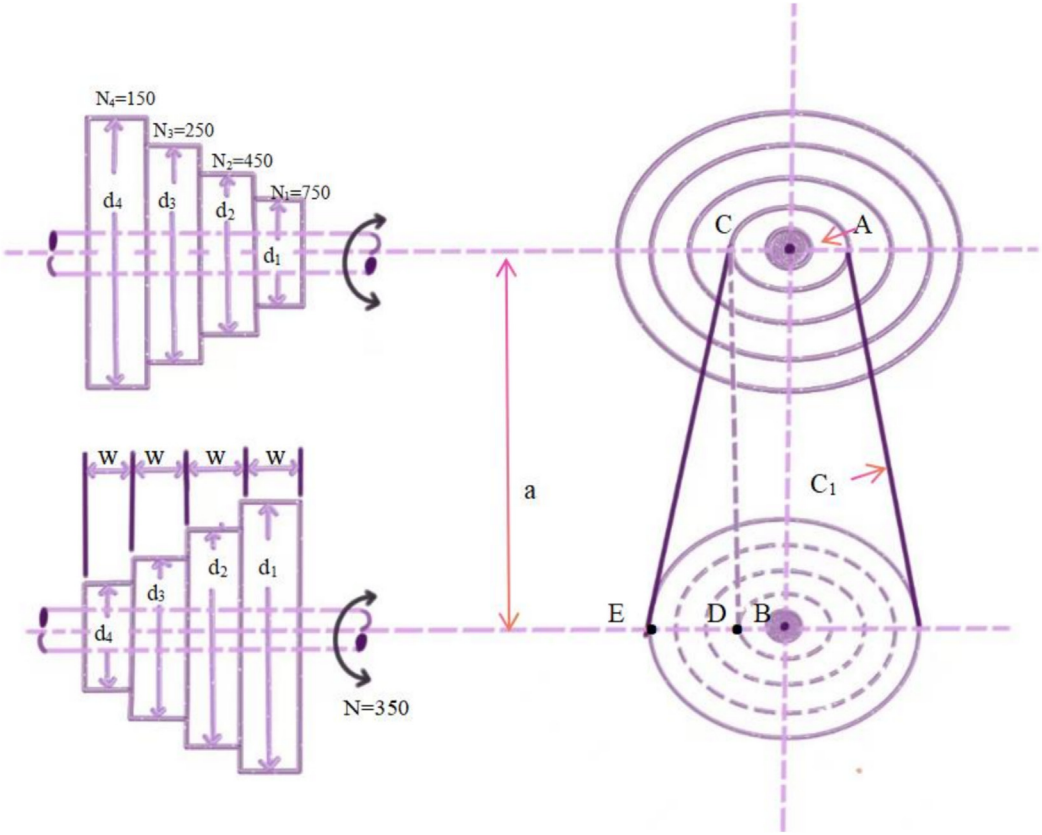

Fig. 18. Schematic view of the step-cone pulley design problem.

Table 18
Comparison outcome for step-cone pulley problem.

Algorithm	Max	Min	Mean	Std	Wilcoxon	Friedman Value
GQPSO	7.09702E + 12	1.92227E + 11	1.79446E + 12	1.33757E + 12	(+)	9.73
TCSPSO	702.2071129	16.56601941	55.79002922	134.0594336	(+)	2.33
MELGWO	690.0626044	17.48013293	69.82866839	123.3621054	(+)	3.40
GWO	79019154.11	3347567.995	28470306.5	20220796.58	(+)	7.10
HHO	108763161.3	18.46193832	21679065.51	30447096.76	(+)	6.43
WOA	3.19487E + 11	17.78660088	21,724,805,937	74,815,684,325	(+)	5.00
RIME	23767196.94	11708.72872	2372146.228	5105479.195	(+)	5.83
CPO	1.8127E + 18	7.82074E + 11	2.98868E + 17	5.44137E + 17	(+)	11.27
NRBO	1.12983E + 11	16.69959624	9,419,219,560	26,259,696,737	(+)	4.23
SWO	1.19697E + 19	68,053,841,545	7.5222E + 17	2.44403E + 18	(+)	10.77
NOA	5.55284E + 16	2.42332E + 11	1.85704E + 15	1.01369E + 16	(+)	10.23
BBO	**297.5027018**	**16.21191219**	**30.49472046**	**51.85089496**	/	**1.67**

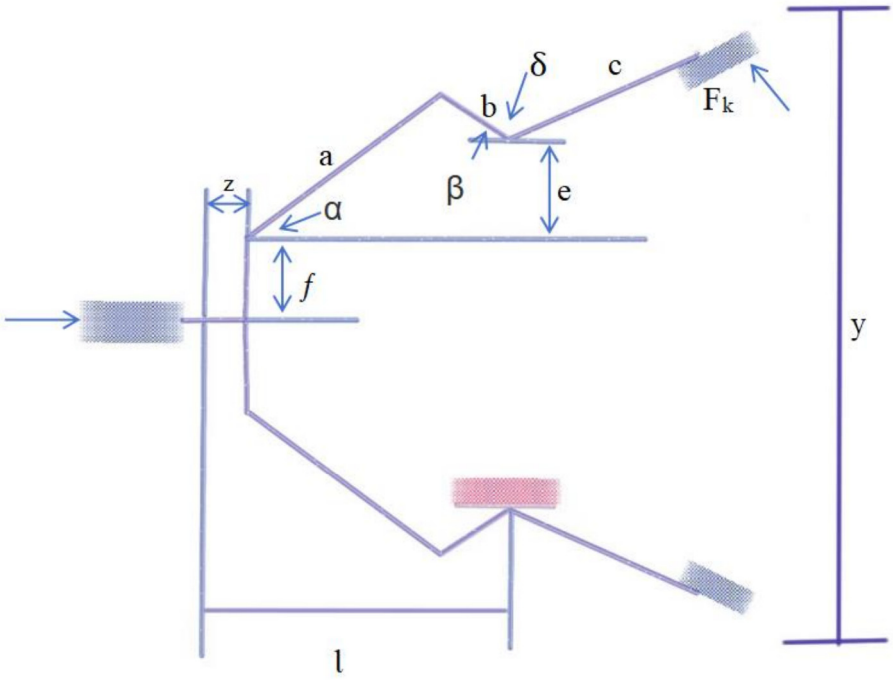

Fig. 19. Schematic view of the Robot gripper design problem.

Table 19
Comparison results for Robot gripper problem.

Algorithm	Max	Min	Mean	Std	Wilcoxon	Friedman Value
GQPSO	2.39933E + 19	259.8414858	6.63124E + 18	6.72712E + 18	(+)	12.00
TCSPSO	6.690058205	**2.550967408**	4.026301702	1.161581086	(−)	3.33
MELGWO	**4.827763085**	2.898231872	**3.554518808**	**0.466114975**	(−)	**2.50**
GWO	5.076519975	2.631415899	3.836403892	0.477893703	(−)	3.70
HHO	81.41855722	3.27665291	23.45213546	25.74750789	(+)	8.17
WOA	64.38852963	3.343932978	9.93566033	13.44047053	(+)	6.60
RIME	6.201663276	2.753051249	4.260751597	0.834107946	(+)	4.23
CPO	2.9861E + 16	6.503260969	1.39058E + 15	5.58555E + 15	(+)	10.10
NRBO	9.226647229	3.033763828	5.460221309	1.520588975	(+)	6.20
SWO	90.51990644	5.529115855	22.95879588	22.94261391	(+)	9.17
NOA	35.03881172	6.174418531	13.18262678	7.411782271	(+)	9.00
BBO	5.24070011	2.85295343	3.73449982	0.532652053	/	3.00

1. Inspired by beavers' self-organizing dam-building behavior, the BBO is proposed as a novel metaheuristic algorithm.
2. Comprehensive validation against 11 MAs (GQPSO, TCSPSO, MELGWO, GWO, HHO, WOA, RIME, CPO, NRBO, SWO, NOA) is conducted using CEC2017 (30D/50D/100D) and CEC2022 (10D/20D) benchmarks.
3. BBO demonstrates superior convergence and stability, evidenced by mean and standard deviation metrics across unimodal, multimodal, and hybrid composition functions.
4. Statistical verification via Wilcoxon signed-rank and Friedman mean rank tests confirms BBO significantly outperforms most competitors, consistently ranking first in Friedman rankings.
5. In real-world applications (photovoltaic parameter design and engineering optimization), BBO achieves better solution metrics than most peers.
6. Statistical analysis shows BBO either dominates competitors or performs comparably to the top algorithm.

Although extensive experimental studies have validated the effectiveness of BBO, there remains room for performance improvement. For instance, in some complex engineering optimization problems, BBO does not demonstrate significant superiority over certain existing algorithms. Future research could consider incorporating mechanisms from other algorithms or proposing novel improvement strategies to enhance BBO's convergence capability in complex real-world optimization problems, such as integrating adaptive population reduction mechanisms or employing reinforcement learning to guide population updates. Additionally, the current study has only focused on continuous single-objective optimization problems. Future work may explore developing discrete versions (e.g., binary version) and multi-objective versions of BBO to investigate its performance on combinatorial optimization and multi-objective optimization problems. Furthermore, potential integration with machine learning algorithms could be considered, including neural architecture search,

neural network parameter optimization, and surrogate model-based data-driven optimization approaches.

Declaration of competing interest

The authors declare that they have no known competing financial interests or personal relationships that could have appeared to influence the work reported in this paper.

References

[1] El-Dabah MA et al. Photovoltaic model parameters identification using Northern Goshawk Optimization algorithm. Energy 2023;262:125522.
[2] Subudhi B, Pradhan R. Bacterial foraging optimization approach to parameter extraction of a photovoltaic module. IEEE Trans. Sustainable Energy 2017;9(1):381–9.
[3] Wang J et al. Photovoltaic cell parameter estimation based on improved equilibrium optimizer algorithm. Energ. Conver. Manage. 2021;236:114051.
[4] Deng L, Liu S. Snow ablation optimizer: a novel metaheuristic technique for numerical optimization and engineering design. Expert Syst. Appl. 2023;225:120069.
[5] Fu S et al. Red-billed blue magpie optimizer: a novel metaheuristic algorithm for 2D/3D UAV path planning and engineering design problems. Artif. Intell. Rev. 2024;57(6):134.
[6] Abdel-Basset M et al. Nutcracker optimizer: a novel nature-inspired metaheuristic algorithm for global optimization and engineering design problems. Knowl.-Based Syst. 2023;262:110248.
[7] Lian JJ et al. Trend-Aware Mechanism for metaheuristic algorithms. Appl. Soft Comput. 2025:113505.
[8] Ouyang K et al. Escape: an optimization method based on crowd evacuation behaviors. Artif. Intell. Rev. 2024;58(1):19.
[9] Rawa M et al. Current-voltage curves of planar heterojunction perovskite solar cells–Novel expressions based on Lambert W function and special Trans Function Theory. J. Adv. Res. 2023;44:91–108.
[10] Houssein EH et al. Optimizing quantum cloning circuit parameters based on adaptive guided differential evolution algorithm. J. Adv. Res. 2021;29:147–57.
[11] Azizi M et al. Shape and size optimization of truss structures by Chaos game optimization considering frequency constraints. J. Adv. Res. 2022;41:89–100.
[12] Heidari AA et al. Harris hawks optimization: Algorithm and applications. Futur. Gener. Comput. Syst. 2019;97:849–72.
[13] Salcedo-Sanz S. Modern meta-heuristics based on nonlinear physics processes: a review of models and design procedures. Phys. Rep. 2016;655:1–70.
[14] Li G et al. Review of the metaheuristic algorithms in applications: visual analysis based on bibliometrics. Expert Syst. Appl. 2024;255:124857.
[15] Hussain K et al. Metaheuristic research: a comprehensive survey. Artif. Intell. Rev. 2019;52(4):2191–233.
[16] Kennedy, J. and R. Eberhart. Particle swarm optimization. in Proceedings of ICNN'95-international conference on neural networks. 1995. ieee.
[17] Kirkpatrick S, Gelatt Jr CD, Vecchi MP. Optimization by simulated annealing. Science 1983;220(4598):671–80.
[18] Holland JH. Genetic algorithms. Sci. Am. 1992;267(1):66–73.
[19] Rao RV, Savsani VJ, Vakharia DP. Teaching–learning-based optimization: a novel method for constrained mechanical design optimization problems. Comput. Aided Des. 2011;43(3):303–15.
[20] Bonabeau, E., M. Dorigo, and G. Theraulaz, *Swarm* intelligence: from natural to artificial systems. 1999: Oxford university press.
[21] Tang J, Liu G, Pan Q. A review on representative swarm intelligence algorithms for solving optimization problems: applications and trends. IEEE/CAA J. Autom. Sin. 2021;8(10):1627–43.
[22] Dorigo M, Stützle T. Ant colony optimization. MIT Press 2004.
[23] Mirjalili S et al. Grey wolf optimizer. Adv. Eng. Softw. 2014;69:46–61.
[24] Xie G et al. Economic-environmental dispatch of isolated microgrids based on dynamic classification sparrow search algorithm. Expert Syst. Appl. 2025;271:126677.
[25] Li G et al. A mixing algorithm of ACO and ABC for solving path planning of mobile robot. Appl. Soft Comput. 2023;148:110868.
[26] Peng L et al. Hierarchical Harris hawks optimizer for feature selection. J. Adv. Res. 2023;53:261–78.
[27] Zhang Z, Han Y. Discrete sparrow search algorithm for symmetric traveling salesman problem. Appl. Soft Comput. 2022;118:108469.
[28] Deng W et al. A novel two-stage hybrid swarm intelligence optimization algorithm and application. Soft. Comput. 2012;16(10):1707–22.
[29] Attiya I et al. An improved hybrid swarm intelligence for scheduling IoT application tasks in the cloud. IEEE Trans. Ind. Inf. 2022;18(9):6264–72.
[30] Mishra VL, Chauhan YK, Verma KS. A new hybrid swarm intelligence-based maximum power point tracking technique for solar photovoltaic systems under varying irradiations. Expert Syst. Appl. 2025;264:125786.
[31] Liu Y, Huang H, Zhou J. A dual cluster head hierarchical routing protocol for wireless sensor networks based on hybrid swarm intelligence optimization. IEEE Internet Things J. 2024;11(9):16710–21.
[32] Wolpert DH, Macready WG. No free lunch theorems for optimization. IEEE Trans. Evol. Comput. 2002;1(1):67–82.
[33] Jordehi AR. Parameter estimation of solar photovoltaic (PV) cells: a review. Renew. Sustain. Energy Rev. 2016;61:354–71.
[34] Xiong G et al. Parameter extraction of solar photovoltaic models using an improved whale optimization algorithm. Energ. Conver. Manage. 2018;174:388–405.
[35] Abdel-Basset M et al. Solar photovoltaic parameter estimation using an improved equilibrium optimizer. Sol. Energy 2020;209:694–708.
[36] Rawat N et al. A new grey wolf optimization-based parameter estimation technique of solar photovoltaic. Sustainable Energy Technol. Assess. 2023;57:103240.
[37] Ebrahimi SM et al. Parameters identification of PV solar cells and modules using flexible particle swarm optimization algorithm. Energy 2019;179:358–72.
[38] Ahmed WAEM et al. Fractional order Darwinian particle swarm optimization for parameters identification of solar PV cells and modules. Alex. Eng. J. 2022;61(2):1249–63.
[39] Brazier RE et al. Beaver: Nature's ecosystem engineers. WIREs Water 2021;8(1):e1494.
[40] Gurnell AM. The hydrogeomorphological e•ects of beaver dam-building activity. Prog. Phys. Geogr.: Earth Environ. 1998;22(2):167–89.
[41] Müller-Schwarze, D., *The Beaver*. Natural History of a Wetlands Engineer. 2011: Cornell University Press.
[42] Law A, McLean F, Willby NJ. Habitat engineering by beaver benefits aquatic biodiversity and ecosystem processes in agricultural streams. Freshw. Biol. 2016;61(4):486–99.
[43] Swinnen KRR et al. Environmental factors influencing beaver dam locations. J. Wildl. Manag. 2019;83(2):356–64.
[44] Busher PE. Food caching behavior of beavers (castor canadensis): selection and use of woody species. Am. Midl. Nat. 1996;135(2):343–8.
[45] Wilcoxon F. Individual comparisons by ranking methods. Biometrics 1945;1(6):80–3.
[46] Friedman M. The use of ranks to avoid the assumption of normality implicit in the analysis of variance. J. Am. Stat. Assoc. 1937;32(200):675–701.
[47] Wu, G., R. Mallipeddi, and P. Suganthan, *Problem Definitions* and Evaluation Criteria for the CEC 2017 Competition and Special Session on Constrained Single Objective Real-Parameter Optimization. 2016.
[48] Biedrzycki, R., J. Arabas, and E. Warchulski. A Version of NL-SHADE-RSP Algorithm with Midpoint for CEC 2022 Single Objective Bound Constrained Problems. in 2022 IEEE Congress on Evolutionary Computation (CEC). 2022.
[49] Coelho LDS. Gaussian quantum-behaved particle swarm optimization approaches for constrained engineering design problems. Expert Syst. Appl. 2010;37(2):1676–83.
[50] Zhang X et al. Terminal crossover and steering-based particle swarm optimization algorithm with disturbance. Appl. Soft Comput. 2019;85:105841.
[51] Ahmed R et al. Memory, evolutionary operator, and local search based improved Grey Wolf Optimizer with linear population size reduction technique. Knowl.-Based Syst. 2023;264:110297.
[52] Mirjalili S, Mirjalili SM, Lewis A. Grey wolf optimizer. Adv. Eng. Softw. 2014;69:46–61.
[53] Mirjalili S, Lewis A. The whale optimization algorithm. Adv. Eng. Softw. 2016;95:51–67.
[54] Su H et al. RIME: a physics-based optimization. Neurocomputing 2023;532:183–214.
[55] Abdel-Basset M, Mohamed R, Abouhawwash M. Crested porcupine optimizer: a new nature-inspired metaheuristic. Knowl.-Based Syst. 2024;284:111257.
[56] Sowmya R, Premkumar M, Jangir P. Newton-Raphson-based optimizer: a new population-based metaheuristic algorithm for continuous optimization problems. Eng. Appl. Artif. Intel. 2024;128:107532.
[57] Abdel-Basset M et al. Spider wasp optimizer: a novel meta-heuristic optimization algorithm. Artif. Intell. Rev. 2023;56(10):11675–738.
[58] Yu K et al. Parameters identification of photovoltaic models using an improved JAYA optimization algorithm. Energ. Conver. Manage. 2017;150:742–53.
[59] Ferreira MP et al. A constrained ITGO heuristic applied to engineering optimization. Expert Syst. Appl. 2018;110:106–24.
[60] Naruei I, Keynia F. A new optimization method based on COOT bird natural life model. Expert Syst. Appl. 2021;183:115352.
[61] Xiong W et al. An effective method for global optimization – improved slime mould algorithm combine multiple strategies. Egyptian Informatics Journal 2024;25:100442.